

University of Alabama in Huntsville

LOUIS

Theses

UAH Electronic Theses and Dissertations

2014

Modal analysis and acoustic transmission through offset-core honeycomb sandwich panels

Adam Dustin Mathias

Follow this and additional works at: <https://louis.uah.edu/uah-theses>

Recommended Citation

Mathias, Adam Dustin, "Modal analysis and acoustic transmission through offset-core honeycomb sandwich panels" (2014). *Theses*. 90.
<https://louis.uah.edu/uah-theses/90>

This Thesis is brought to you for free and open access by the UAH Electronic Theses and Dissertations at LOUIS. It has been accepted for inclusion in Theses by an authorized administrator of LOUIS.

**MODAL ANALYSIS AND ACOUSTIC TRANSMISSION
THROUGH OFFSET-CORE HONEYCOMB SANDWICH
PANELS**

by

ADAM DUSTIN MATHIAS

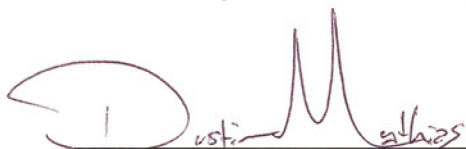
A THESIS

Submitted in partial fulfillment of the requirements
for the degree of Master of Science in Engineering
in
The Department of Mechanical and Aerospace Engineering
to
The School of Graduate Studies
of
The University of Alabama in Huntsville

HUNTSVILLE, ALABAMA

2014

In presenting this thesis in partial fulfillment of the requirements for a master's degree from The University of Alabama in Huntsville, I agree that the Library of this University shall make it freely available for inspection. I further agree that permission for extensive copying for scholarly purposes may be granted by my advisor or, in his/her absence, by the Chair of the Department or the Dean of the School of Graduate Studies. It is also understood that due recognition shall be given to me and to The University of Alabama in Huntsville in any scholarly use which may be made of any material in this thesis.

A handwritten signature in red ink, appearing to read "Adam Dustin Mathias", written over a horizontal line.


Adam Dustin Mathias

2014/05/09
(date)

THESIS APPROVAL FORM

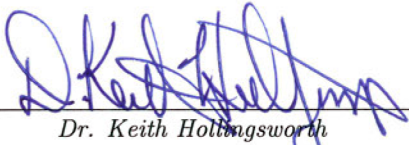
Submitted by Adam Dustin Mathias in partial fulfillment of the requirements for the degree of Master of Science in Engineering in Aerospace Engineering and accepted on behalf of the Faculty of the School of Graduate Studies by the thesis committee.

We, the undersigned members of the Graduate Faculty of The University of Alabama in Huntsville, certify that we have advised and/or supervised the candidate of the work described in this thesis. We further certify that we have reviewed the thesis manuscript and approve it in partial fulfillment of the requirements for the degree of Master of Science in Engineering in Aerospace Engineering.



_____ 5/2/14 Committee Chair
Dr. Kader Frendi (Date)


_____ 5/2/14
Dr. Jason Cassibry (Date)


_____ 5/2/14
Dr. Sivaguru Ravindran (Date)


_____ 5/9/14 Department Chair
Dr. Keith Hollingsworth (Date)


_____ 05/22/14 College Dean
Dr. Shankar Mahalingam (Date)


_____ 6/3/14 Graduate Dean
Dr. David Berkowitz (Date)

ABSTRACT

School of Graduate Studies
The University of Alabama in Huntsville

Degree Masters of Science College/Dept. Engineering/Mechanical and
in Engineering Aerospace Engineering

Name of Candidate Adam Dustin Mathias

Title Modal Analysis and Acoustic Transmission
Through Offset-core Honeycomb Sandwich Panels

The work presented in this thesis is motivated by an earlier research that showed that double, offset-core honeycomb sandwich panels increased thermal resistance and, hence, decreased heat transfer through the panels. This result led to the hypothesis that these panels could be used for acoustic insulation. Using commercial finite element modeling software, COMSOL Multiphysics, the acoustical properties, specifically the transmission loss across a variety of offset-core honeycomb sandwich panels, is studied for the case of a plane acoustic wave impacting the panel at normal incidence. The transmission loss results are compared with those of single-core honeycomb panels with the same cell sizes. The fundamental frequencies of the panels are also computed in an attempt to better understand the vibrational modes of these particular sandwich-structured panels. To ensure that the finite element analysis software is adequate for the task at hand, two relevant benchmark problems are solved and compared with theory. Results from these benchmark results compared well to those obtained from theory. Transmission loss results from the offset-core honeycomb sandwich panels show increased transmission loss, especially for large cell honeycombs when compared to single-core honeycomb panels.

Abstract Approval: Committee Chair



Dr. Kader Frendi

Department Chair



Dr. Keith Hollingsworth

Graduate Dean



Dr. David Berkowitz

ACKNOWLEDGMENTS

I would like to thank my advisor, Dr. Kader Frendi, for increasing my interest in acoustics through formal lecture and during our meetings. It was his acoustics class that helped me decide to research an acoustics topic for this thesis. Dr. Frendi has shown the utmost patience throughout this process, and I have a significant amount of respect for him.

Also, I would like to thank my committee, Dr. Jason Cassibry and Dr. Sivaguru Ravindran, for asking thoughtful questions and for providing feedback for the thesis work. Secondly, I want to thank Dr. James Blackmon for his helpful discussions about offset-core honeycomb panels.

Laura Barkett, a fellow student and study partner, has also contributed a significant amount of her time talking through problems with me even though they were not hers to solve. She has always been there, by my side, through the years. For that friendship, I want to thank her.

I would also like to thank my late friend and co-worker, Dr. Jeremy Galusha, for giving me helpful advice and for encouraging me as I worked toward this milestone in my career. Our discussions about science, throughout the years, have helped me to have a better understanding of the work that we performed together.

Most importantly, I want to thank my wife, Karina. Without my wife's support, it would have been difficult, if not impossible, to pursue higher level education.

TABLE OF CONTENTS

	PAGE
List of Figures	x
List of Tables	xiii
List of Symbols	xv
Chapter	
1 Introduction	1
1.1 Problem Statement and Goals	1
1.2 Outline	3
2 Background Information	4
2.1 Overview	4
2.1.1 Applications of Sandwich-structured Panels	4
2.1.2 Efforts to Optimize Noise Reduction	4
2.1.3 Description of Single-core Honeycomb Panels	5
2.1.4 Description of Offset-core Honeycomb Panels	7
2.2 Vibration and Noise Reduction Metrics	9
3 Methodology	11
3.1 Overview of the Finite Element Method	11
3.2 COMSOL Multiphysics	13

3.3	Model Development	14
3.4	Benchmarking	15
3.4.1	Theory for the Natural Frequencies of a Rectangular Plate . .	18
3.4.2	Theory for Transmission Loss through a Rectangular Plate . .	20
3.5	Acoustic Transmission through a Sandwich Panel	23
3.6	Finite Element Analysis of Honeycomb Sandwich Panels	24
3.6.1	Modal Analysis	27
3.6.2	Transmission Loss	28
3.6.3	Material Properties and Boundary Conditions	30
3.6.4	Mesh	34
3.6.5	Solver	38
4	Results and Discussion	40
4.1	Benchmarking Results	40
4.1.1	Results of Modal Analysis	40
4.1.2	Results of Acoustic Transmission Loss Study	42
4.2	Modal Analysis of Honeycomb Panels	43
4.2.1	Single-core Honeycomb Panel	44
4.2.2	Offset-core Honeycomb Panels	48
4.3	Transmission Loss of Honeycomb Panels	53
5	Conclusion	64
6	Recommendations	66

APPENDIX A: Modal Analysis of a Rectangular Plate	69
APPENDIX B: Modal Analysis for Honeycomb Sandwich Panels	72
APPENDIX C: Sound Transmission Loss Through a Rectangular Plate	78
REFERENCES	80

LIST OF FIGURES

FIGURE	PAGE
1.1 3D solid model of a single-core honeycomb sandwich panel.	2
2.1 3D solid model of an offset-core honeycomb sandwich panel	7
2.2 Geometry of honeycomb-core cells	8
2.3 Two honeycomb cores offset from one another	9
3.1 Case I: A simply supported plate – lower four edges have a prescribed displacement equal to zero	16
3.2 Case II: A simply supported plate between two air domains	17
3.3 Plane wave radiation from the top boundary toward the aluminum plate	17
3.4 Panel response from excitation with a plane wave at $f = 6,800\text{Hz}$. .	18
3.5 A graphical representation of an acoustic wave impinging upon an offset-core honeycomb panel at normal incidence	23
3.6 A transparent view of a single-core honeycomb panel	25
3.7 A transparent view of a offset-core honeycomb panel in which the core layers are vertically offset	26
3.8 Fixed boundaries of a single-core honeycomb panel	31
3.9 Fixed boundaries of an offset-core honeycomb panel	31
3.10 Plane wave radiation toward offset-core honeycomb panel	32
3.11 Physics-driven free tetrahedral mesh applied to an offset-core honeycomb sandwich panel	35
3.12 Detail view of a free tetrahedral mesh applied to an offset-core honeycomb sandwich panel	36

3.13	Free tetrahedral meshing of air domains and honeycomb panel for transmission loss studies	36
3.14	Mesh parameter setup within the COMSOL Multiphysics environment	37
4.1	Displacement field plot for the fundamental mode of a rectangular plate ($f_n = 41.79\text{Hz}$)	41
4.2	Comparison of theory to FEA results for the natural frequencies of a solid aluminum plate	41
4.3	Comparison of theory to FEA results for the transmission loss through a solid aluminum plate	42
4.4	Detailed view of Figure 4.3 for $f = 0\text{Hz}$ to 1kHz	43
4.5	Detailed view of Figure 4.3 for $f = 1\text{kHz}$ to 10kHz	43
4.6	Response of a 2in. x 3in. single-core panel with 1in. cell size	45
4.7	Response of a 2in. x 3in. single-core panel with 0.75in. cell size	45
4.8	Response of a 2in. x 3in. single-core panel with 0.50in. cell size	46
4.9	Response of a 4in. x 6in. single-core panel with 1in. cell size	46
4.10	Response of a 8in. x 12in. single-core panel with 1in. cell size	47
4.11	Mode shape of a 4in. x 6in. offset-core panel with 1in. cell size	49
4.12	Response of a 2in. x 3in. offset-core panel with 1in. cell size	50
4.13	Response of a 2in. x 3in. offset-core panel with 0.75in. cell size	50
4.14	Response of a 2in. x 3in. offset-core panel with 0.50in. cell size	51
4.15	Response of a 4in. x 6in. offset-core panel with 1in. cell size	51
4.16	Response of a 8in. x 12in. offset-core panel with 1in. cell size	52
4.17	Sound pressure level on a 2in. x 3in. single-core panel with 1in. cell size	55
4.18	Sound pressure level on a 2in. x 3in. offset-core panel with 1in. cell size)	55

4.19	Sound pressure level on a 2in. x 3in. single-core panel with 0.75in. cell size)	56
4.20	Sound pressure level on a 2in. x 3in. offset-core panel with 0.75in. cell size)	56
4.21	Sound pressure level on a 2in. x 3in. single-core panel with 0.50in. cell size)	57
4.22	Sound pressure level on a 2in. x 3in. offset-core panel with 0.50in. cell size)	57
4.23	Sound pressure level comparison for 2in. x 3in. panels with 1in. cell sizes)	58
4.24	Sound pressure level comparison for 2in. x 3in. panels with 0.75in. cell sizes)	58
4.25	Sound pressure level comparison for 2in. x 3in. panels with 0.50in. cell sizes)	59
4.26	Sound pressure level comparison for single-core panels	59
4.27	Sound pressure level comparison for offset-core panels	60
4.28	Comparison of transmission loss for 2in. x 3in. single-core and offset-core panels with 1in. cell size	60
4.29	Comparison of transmission loss for 2in. x 3in. single-core and offset-core panels with 0.75in. cell size	61
4.30	Comparison of transmission loss for 2in. x 3in. single-core and offset-core panels with 0.50in. cell size	61
4.31	Comparison of transmission loss for single-core panels	62
4.32	Comparison of transmission loss for offset-core panels	62

LIST OF TABLES

TABLE	PAGE
3.1 Single-core Panel Geometries	27
3.2 Offset-core Panel Geometries	27
3.3 Mesh Elements for Each Natural Frequency Study	38
3.4 Mesh Elements for Each Transmission Loss Study	38
4.1 Fundamental Frequencies of Single-core Honeycomb Panels	44
4.2 Fundamental Frequencies of Offset-core Honeycomb Panels	48
4.3 Transmitted Overall Sound Pressure Level	63
A.1 Matlab Output for $f(i,j)$	70
A.2 COMSOL Output for $f(i,j)$	70
A.3 Percent Error Between Theory and COMSOL Results for $f(i,j)$	70
A.4 Displacement Plots for COMSOL Output of Natural Frequencies $f(i,j)$	71
B.1 Displacement Field Plots for COMSOL Output of Eigenmodes for Off- set Honeycomb $f(i,j)$	73
B.2 Natural Frequencies for Single-core Honeycomb Sandwich Panels - 2in. x 3in.	74
B.3 Natural Frequencies for Offset-core Honeycomb Sandwich Panels - 2in. x 3in.	75
B.4 Natural Frequencies for Single-core Honeycomb Sandwich Panels - 1in. Cell Size	76

B.5	Natural Frequencies for Offset-core Honeycomb Sandwich Panels - 1in.	
	Cell Size	77

LIST OF SYMBOLS

SYMBOL	DEFINITION
Latin	
a	Length of solid or sandwich panel [m]
b	Width of solid or sandwich panel [m]
c	Speed of sound [m/s]
c_{air}	Speed of sound in air [m/s]
c_{al}	Speed of sound in aluminum [m/s]
D	Flexural rigidity [Pa · m ³]
d	Length of honeycomb cell wall [m]
E	Young's modulus [Pa]
f	Frequency [Hz]
f_c	Center frequency [Hz]
Δf	Frequency bandwidth [Hz]
f_l	Lower frequency in band [Hz]
f_n	Fundamental frequency [Hz]
f_u	Upper frequency in band [Hz]
h	Thickness of a solid or sandwich panel [m]

h_{al}	Thickness of a rectangular aluminum plate [m]
h_c	Thickness of a honeycomb core [m]
I	Intensity [Watts/m ²]
I_I	Transmitted intensity [Watts/m ²]
I_T	Incident intensity [Watts/m ²]
i	Mathematical index
j	Mathematical index
k	Wave number
L_p	Sound Pressure Level [dB]
L_T	Overall Sound Pressure Level [dB]
m	Mass [grams]
p	Overall Sound Pressure Level [dB]
p	Pressure [Pa]
p_b	Background pressure field [Pa]
p_i	Incident pressure wave [Pa]
p_r	Reflected pressure wave [Pa]
p_s	Scattered pressure field [Pa]
p_t	Transmitted pressure wave [Pa]
p_{tot}	Total pressure [Pa]

Q_i	Monopole source [$1/s^2$]
q_d	Dipole source [N/m^3]
r	Impedance [$Pa \cdot s/m$]
r_{air}	Impedance of air [$Pa \cdot s/m$]
r_{al}	Impedance of aluminum [$Pa \cdot s/m$]
S	Distance between hexagonal cell walls [m]
S_T	Total cell size [m]
T	Temperature [K]
T_I	Intensity transmission coefficient
TL	Transmission Loss [dB]
t	Time [s]
t_c	Thickness of honeycomb cell wall [m]
t_f	Thickness of face plate [m]
W	Eigenfunction or mode shape
w	Transverse displacement or lateral deflection
x	X-direction
y	Y-direction
z	Z-direction

Greek

Δ_T	Laplace operator in the tangent plane at a point
∇	Del operator
γ	Mass density [grams/m ²]
ω	Angular frequency or radian frequency [rad/s]
Π	Power [Watts]
Π_I	Incident power [Watts]
Π_T	Transmitted power [Watts]
π	Pi
ρ	Density [grams/m ³]
ρ_{air}	Density of air at standard temperature and pressure [grams/m ³]
ρ_{al}	Density of aluminum [grams/m ³]
ν	Poisson's ratio

Vectors and Complex Values

\mathbf{k}	Wave vector
\mathbf{n}	Unit normal vector
\mathbf{P}_i	Complex pressure amplitude of an incident wave [Pa]
\mathbf{P}_r	Complex pressure amplitude of a reflected wave [Pa]
\mathbf{P}_t	Complex pressure amplitude of a transmitted wave [Pa]

\mathbf{r}	Location on the boundary
\mathbf{u}	Displacement field [m]
$\hat{\mathbf{x}}$	The x unit vector, indicating that a parameter/quantity is in the x-direction.
$\hat{\mathbf{y}}$	The y unit vector, indicating that a parameter/quantity is in the y-direction.
$\hat{\mathbf{z}}$	The z unit vector, indicating that a parameter/quantity is in the z-direction.

Acronyms

BC	Boundary Condition
FEA	Finite Element Analysis
FEM	Finite Element Method
FGMRES	Flexible Generalized Minimal Residual Method
GMRES	Generalized Minimal Residual Method
MUMPS	Multifunctional Massively Parallel Sparse Direct Solver
OCHP	Offset-core Honeycomb Panel
PDE	Partial Differential Equation
SCHP	Single-core Honeycomb Panel
SPL	Sound Pressure Level
TL	Transmission Loss

Typography

Bold Bold type is used to identify vectors — that is, quantities that have both magnitude and direction, and, in Cartesian coordinates, consist of x, y, and z components. It is also used to display complex values.

For Katrina, Skylar, and Lyra

CHAPTER 1

INTRODUCTION

1.1 Problem Statement and Goals

By understanding the vibrational and acoustical properties of a material with numerical techniques such as the finite element method (FEM), one can learn how to approach the problem of suppressing unwanted vibration or transmittance of sound at certain frequencies. By correctly designing and analyzing sandwich panels with FEM, one could potentially design optimized aircraft-lining panels that reduce the propagation of engine noise into the cabin.

Modern sandwich-structured panels are composed of a thick core that is light weight and consists of low to moderate stiffness, interposed between two sheet metal, fiberglass, or carbon fiber face plates. Previous studies have shown that, due to impedance mismatch at the interface of adjoining media, sound waves witness an inefficient energy transfer when traveling across that interface [1]. An acoustic wave traveling, at normal incidence, toward a single-core sandwich panel would need to pass through the face plate, the core material, and a second face plate. A double-core sandwich panel would behave similarly when impacted by an acoustic wave, but in the case that one core is offset from the other, more opportunity to impede the

acoustic wave would seemingly arise due to the variety of geometries that would reflect the traveling wave. A 3D solid model representation of a single-core honeycomb sandwich panel, with the top face plate lifted so that the core can be seen, is shown in Figure 1.1.

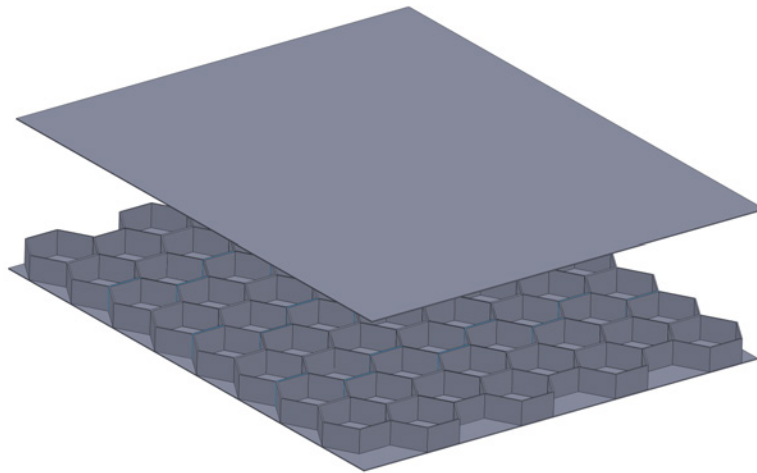


Figure 1.1: 3D solid model of a single-core honeycomb sandwich panel.

Single-core honeycomb panels (SCHP) have been a topic of research for decades, but double-core honeycomb sandwich panels, in which the cores are offset, have been recently developed [2]. The goal of the current research is to study the vibro-acoustic properties of various offset-core honeycomb panels (OCHP), specifically, the transmittance of sound through the panels across a broadband frequency range, and compare the results to those of the single-core honeycomb sandwich panels. As well as studying the sound transmission through the panels, the vibrational modes of the panels are computed and discussed.

1.2 Outline

An overview of the applications of honeycomb panels and previous relevant work with honeycomb sandwich panels is provided in Chapter 2. Chapter 2 also provides a short discussion of some vibrational and noise measurement metrics of sandwich panels. Chapter 3 is a discussion of the finite element method, COMSOL Multiphysics, methods used to benchmark COMSOL Multiphysics, some theory, and the development of the finite element models. This includes details on the geometry of the models, material properties, boundary conditions, and mesh construction. The results, and discussions of the coupled-physics modeling, are presented in Chapter 4. Conclusions about the results, from each type of analysis, are presented in Chapter 5. A brief discussion of recommendations for future studies is presented in Chapter 6. Appendix A contains Matlab code and tabulated data from the modal analysis of the rectangular plate benchmark problem. Appendix B contains tabulated data from the finite element modal analysis of honeycomb sandwich panels. Appendix C contains Matlab code for the rectangular plate sound transmission loss benchmark problem.

CHAPTER 2

BACKGROUND INFORMATION

2.1 Overview

2.1.1 Applications of Sandwich-structured Panels

In applications where weight is a concern, such as aeronautical structures, race cars, satellites, marine craft, and high speed trains, sandwich-structured composite panels are often used. Within the aerospace industry, in particular, single-core honeycomb sandwich panels are used in aircraft ailerons, spoilers, bulkheads, passenger floors, fuselage skins, nacelles, rotor blades, engine intake barrel panels, and wings [3]. These multilayer panels are typically used due to their high strength-to-weight ratio, superior insulation qualities, and lack of corrosion [4] [5]. Reducing fuel consumption while increasing the load capacity is also a driver for the increased use of composite sandwich-structured panels in aerospace industry [6].

2.1.2 Efforts to Optimize Noise Reduction

Previous experimental studies have indicated that the engine noise, transmitted through the aircraft sidewall, is one of the dominant sources of sound transmission into an aircraft cabin [7]. Studies have been done, in recent years, to help suppress

noise that propagates from engine nacelles [8]. More general optimization studies of cylindrical shells, with the intent to minimize the sound transmission into the interior, have also been conducted [9]. In recent years studies on fluid-structure-sound interactions have increased significantly due to an increase in computational power as well as the need to understand the sources of interior cabin noise and propose ways to control them [10] [11] [12] [13] [14] [15] [16] [17] [17] [18] [19] [20]. Other investigations have used finite element analysis (FEA) to conduct parametric studies of honeycomb composite fuselage panels in an attempt to reduce acoustic transmission into an aircraft compartment [21].

The acoustic performance and damping of honeycomb panels has been explored as early as 1959 [22]. By understanding how honeycomb panels transmit sound, engineers can work to optimize the panel using damping. Damping of honeycomb panels to improve sound transmission loss (TL) properties has been studied recently [23]. Passive damping of honeycomb structures using energy absorbing foam has been explored [24]. Active vibration control with piezoelectric panels has also been studied with FEA in an attempt to reduce residual noise in the low to mid-frequency range [25].

2.1.3 Description of Single-core Honeycomb Panels

A single-core honeycomb sandwich panel is constructed of two thin face plates that are separated by a load-carrying core material. Often, these face plates are made of high tensile steel, aluminum alloys, titanium, fiberglass, carbon fiber, or other composites. The structural efficiency provided by sandwich panels is primarily due to the

fact that the face plates carry the bending loads, as the honeycomb core, itself, has a bending modulus that is assumed to be zero, i.e., it does not resist bending [26]. The core, however, significantly stiffens the face plates, and the moment of inertia of the entire panel is increased. It has been determined in previous work that the honeycomb-structured panels increase noise reduction in the low frequency regime, but the stiffness of the core has a negligible effect on attenuation of low frequency noise reduction [7]. Most commonly, honeycomb cores are made of aluminum, impregnated glass, paper, or fiber-reinforced polymers [27].

High modulus, high strength adhesives that come in liquids, pastes, or dry films, rigidly attach the face plates to the core material. To achieve a good bond between the face plates and the honeycomb core by ensuring that the adhesives stay on the honeycomb cell edge, rather than running down the cell walls during the cure cycle, adhesives that have the right rheology must be chosen [28]. Adhesives could potentially play a role in the way that sandwich panels are attached to other panels, as well. Authors have shown, for instance, that using a high strength epoxy to attach honeycomb sandwich panels to the interior of skin subpanels can increase low frequency TL [29].

The benefits of modern honeycomb sandwich panels, including the ones discussed earlier, are:

- Attenuation of sound at certain frequencies
- Resistance to fatigue, fire, and impact damage
- Durability
- High strength-to-weight ratio

- Rigidity
- Insulative with tailorable heat transfer properties
- Manufacturability

2.1.4 Description of Offset-core Honeycomb Panels

The single-core honeycomb sandwich panel is a fairly mature technology, but the offset-core honeycomb sandwich panel is a relatively new concept [2]. The offset-core sandwich panel is comprised of two face plates that are separated by honeycomb core layers that are stacked in an offset arrangement, and it is the focus of the current research. An image of a 3D solid model of an offset-core honeycomb sandwich panel is shown in Figure 2.1. The length of the honeycomb panel, the width of the honeycomb panel, the total thickness of the sandwich panel, the thickness of the honeycomb core, and the thickness of the face plates are shown in Figure 2.1 as a , b , h , h_c , and t_f , respectively.

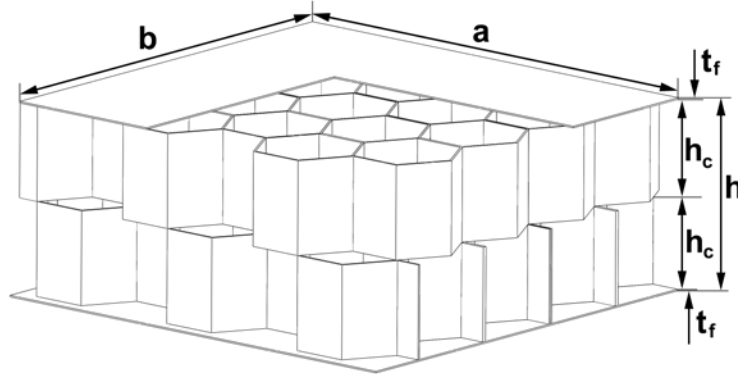


Figure 2.1: 3D solid model of an offset-core honeycomb sandwich panel

The cells of sandwich panels are typically hexagonal or columnar. A core that consists of thin foils in the form of hexagonal cells that are perpendicular to the face plates, however, is the most common [26]. The core is regularly made of aluminum or a polymer. The cellular shape, for the metallic cores, is fabricated by extruding, welding, brazing, and bonding. An image of two honeycomb core unit cells is shown in Figure 2.2. The total cell size, distance between hexagonal cell walls, the thickness of the honeycomb cell wall, and the length of the honeycomb cell wall are shown in Figure 2.2 as S_T , S , t_c , and d , respectively.

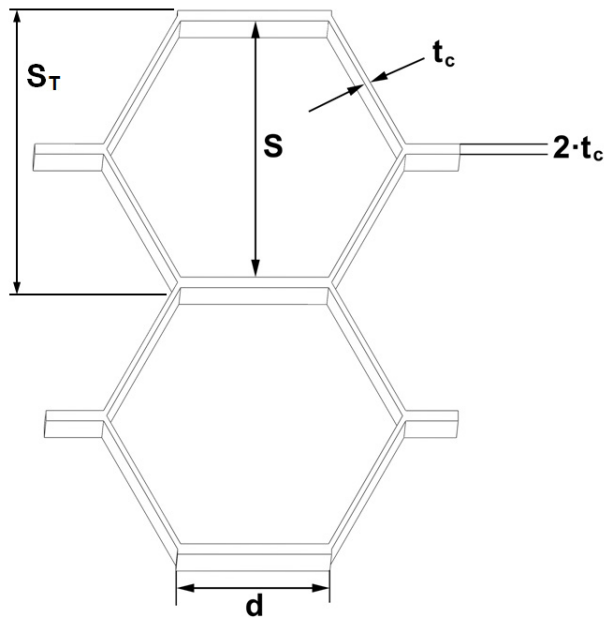


Figure 2.2: Geometry of honeycomb-core cells

An image of an actual offset-core honeycomb is shown in Figure 2.3.



Figure 2.3: Two honeycomb cores offset from one another

2.2 Vibration and Noise Reduction Metrics

The natural frequencies, f_{ij} , of a structure are often considered in vibration problems. If a panel is acted on by an external force, displaced, and then released, it will vibrate at its natural frequencies. The fundamental frequency, or lowest frequency, f_n , is often used when investigating better ways to damp a structure [30]. Knowing these values for honeycomb panels would potentially allow engineers to design panels that vibrate less when impacted by incident sound waves.

Increasing the transmission loss of sandwich panels, especially in the low and middle frequencies due to the reduced damping, is a difficult problem, but ensuring a high transmission loss across a wide bandwidth is the goal of some design engineers [31]. The acoustic performance of a panel has been described by many methods. However, sound transmission loss and power radiation are two standard metrics for determining acoustic performance of the panel [32] [33]. The equations for sound transmission loss of a panel are defined in the Methodology chapter.

Similar properties, the incident sound pressure level (SPL) and transmitted SPL for a panel are useful for describing, relative to a reference sound pressure, the amount that an effective local pressure field deviates from the ambient pressure field. The overall sound pressure level (OASPL) that is transmitted through a panel, a single value, is also useful, as it represents an intensity of the spectrum in its entirety. These terms are described further in the Transmission Loss section of the Methodology chapter.

CHAPTER 3

METHODOLOGY

3.1 Overview of the Finite Element Method

Numerical solutions to many engineering problems, for which analytical solutions are difficult or impossible to obtain, can be found using FEM, also known as FEA. Finite element analysis is advantageous when solving problems with complicated geometries, loadings, boundary conditions, or material properties. The process of discretization, dividing a continuous geometry or domain into smaller elements, allows for an equivalent, mathematically discrete system to be formed. Domain definition, element type, element material properties, element geometric properties, element connectivity, and physical constraints are all defined during the preprocessing phase of FEA. These definitions are then used to compute the primary field variables, i.e., the unknown values of the dependent variables of interest that are governed by the differential equation. The typical process when performing finite element analysis is:

- The partial differential equations (PDE) that need to be solved are first chosen, i.e. the correct representative physics used.
- The geometry for the set of PDE's to be solved is modeled and defined.

- The material properties are applied to the geometry.
- The boundary conditions and initial conditions are applied to the boundaries of the geometry.
- The mesh type is chosen, applied to the geometry, and then refined to suit the problem at hand.
- A solver type that is suited for the problem at hand is chosen.
- The solution is computed, and post-processing is performed on the data obtained.

Previous work has shown, through validation by experimental modal analyses and transmission loss (TL) testing, that FEA is an acceptable method for analyzing the sound TL across complex structures like honeycomb sandwich panels in the low to mid frequency range [34]. This method is also used to study other behaviors of sandwich-structured panels. For instance, other authors have approximated the global behavior of thin composite aircraft sandwich panels by using shell finite elements [35]. The effect of core thickness on the natural frequencies of single-core honeycomb panels has been studied both experimentally and with FEM [36]. Some authors have studied the vibratory behaviors of delaminated honeycomb panels, and the natural frequencies were calculated for panels with varied boundary conditions using the commercial FEM software MSC/NASTRAN [37]. Still, others have studied the linear elastic mechanical properties of honeycomb core structures experimentally and compared their findings to the results from FEA [38]. COMSOL Multiphysics, in particular, has been shown to have relatively high accuracy for eigenfrequency analysis

and sound-structure interaction when compared with analytical and experimental results [39].

3.2 COMSOL Multiphysics

COMSOL Multiphysics is a FEA solver and simulation software package that was originally known as FEMLAB. The present research takes advantage of modules in COMSOL Multiphysics to successfully couple physical phenomena, in particular, the acoustic-structure interaction that occurs when a propagating acoustic wave comes in contact with, and causes vibrations throughout, a structure. These vibrations are then relayed back to the fluid domain as a normal acceleration across the fluid-solid boundary. The term vibro-acoustic system could be used due to the coupling between structural vibrations and the acoustic field.

COMSOL Multiphysics is chosen, also, due to its robust structural mechanics module that allows for deformation analysis with geometric non-linearity. This module is used primarily to perform the modal analysis of the honeycomb sandwich panels. If desired, one could also utilize this module to better understand the stress and strain that occurs within honeycomb sandwich panels that are being impinged by an acoustic wave.

COMSOL Multiphysics utilizes a "free mesher" for 1D, 2D, and 3D geometries. The free mesher allows a user to apply an unstructured tetrahedral, hexahedral, prism, or pyramid mesh to domains, while boundaries are discretized into boundary elements that are triangular or quadrilateral. Mesh element endpoints are known as mesh vertices, and edges are discretized into "edge elements". Rather than manually

meshing each interval of a domain or each boundary individually, COMSOL uses a physics-induced meshing sequence that applies the mesh to the model based on the physics settings that are chosen. For instance, a finer mesh is applied for fluids models than for solid mechanics models.

3.3 Model Development

Solid Works 2010 was used to develop the single-core and offset-core honeycomb sandwich plate models. First, for the single-core honeycomb panel, a honeycomb cell was drawn and dimensioned on a work plane using the hexagonal patterning tool in Solid Works. The shape was extruded to form a single 3D cell. The cell was then placed into an assembly and mated to exact replicas of itself until the desired horizontal and vertical core size for each panel size was obtained. Face plates were drawn and dimensioned on a work plane using the rectangular drawing tool, and then they were extruded to the desired thickness. The face plates were added to the assembly, and they were then mated with the core that was previously created. Mated cells that extended past the length and width of the face plate were subsequently removed using the extruded cut tool within Solid Works.

Offset-core honeycomb panels were created in a similar fashion as the single-core honeycomb panels. However, in this case, two cores were assembled and mated together. One core was vertically offset from the other by half of the distance between cell walls plus the cell wall thickness. The models were saved in a standard exchange format, .STEP, and then imported into COMSOL Multiphysics.

Within the COMSOL Multiphysics software, material properties and boundary conditions were applied to the imported solid model. Solid flat plates, however, were created and analyzed directly within the COMSOL Multiphysics environment rather than being imported from Solid Works 2010. After applying the boundary conditions, the models were meshed, solvers were setup, and the results were computed. The computations were carried out on a x64 based PC with an Intel Core i7-2600k CPU @ 3.40GHz with hyperthreading technology, 4 cores, 8 logical processors, 32GB of random access memory, and an ATI Radeon HD 5700 series graphics card.

3.4 Benchmarking

To validate that COMSOL Multiphysics is suitable for performing the computations necessary for modal analysis and transmission loss studies, two test cases were explored. The idea here is to solve problems for which the solutions are known, and then model a more complex structure in a similar fashion. In the first case, the eigenfrequencies and eigenmodes are found for a solid aluminum plate that is the size of a typical aircraft panel, 16 in. in length, a , 12 in. in width, b , and 0.04 in. in thickness, h . In the second case, frequency-dependent TL is determined for a solid aluminum plate that is surrounded by air on both sides and excited by an acoustic plane wave at normal incidence.

The plates for both scenarios are simply supported. That is, they have a prescribed displacement equal to zero in the direction normal to the plate along the four bottom edges, and they are free everywhere else. The simply supported edges of the plate described for the first case are highlighted in blue in Figure 3.1.

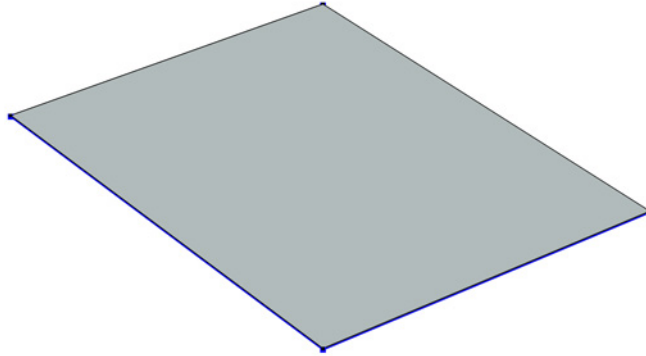


Figure 3.1: Case I: A simply supported plate – lower four edges have a prescribed displacement equal to zero

The solid plates were assumed to behave as linear elastic materials. The plates are set as standard aluminum with a density, ρ_{al} , of 2700kg/m^3 , a Young's modulus, E , of 70GPa , a Poisson's ratio of 0.33 , and a speed of sound, c_{al} , of 6420m/s . The air domains that are used in the second case have a speed of sound, c_{air} , of 343.2m/s , and a density, ρ_{air} , of 1.2754kg/m^3 .

The plate, sandwiched between two air domains, as described in the second case, is shown in Figure 3.2. A plane wave, at $f = 6,800\text{Hz}$, with a pressure amplitude of 20Pa radiates from the topmost boundary as shown in Figure 3.3. The transmitted pressure is much lower than the incident pressure, at this frequency, as indicated by the color bar. The boundaries surrounding the plate are set to the impedance value for air, a r_{air} of $411.6\text{Pa}\cdot\text{s/m}$. The five slices in Figure 3.3 indicate that the

plane wave is well resolved and has minimal reflection from the walls of the air domain when using these boundary conditions. Figure 3.4 shows the panel's response to the excitation by the plane wave in Figure 3.3. In both cases, the models were processed in COMSOL Multiphysics, and the numerical results from the FEA were compared with the results from theory. The results for the benchmark models are shown in the Results chapter.

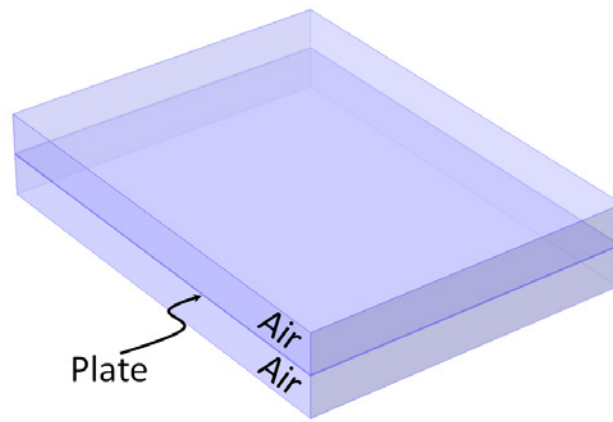


Figure 3.2: Case II: A simply supported plate between two air domains

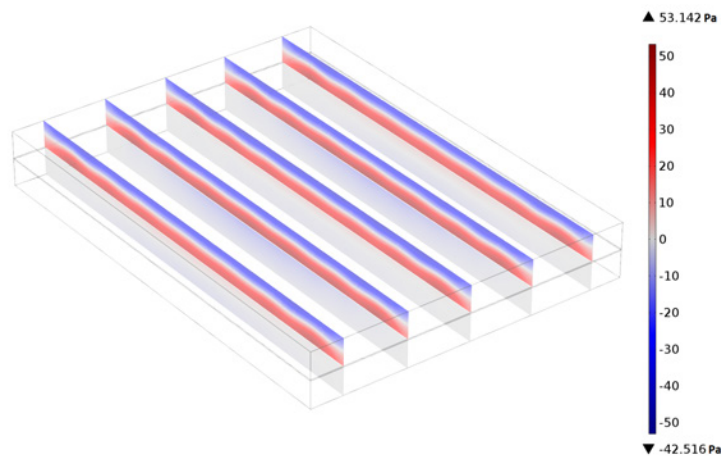


Figure 3.3: Plane wave radiation from the top boundary toward the aluminum plate

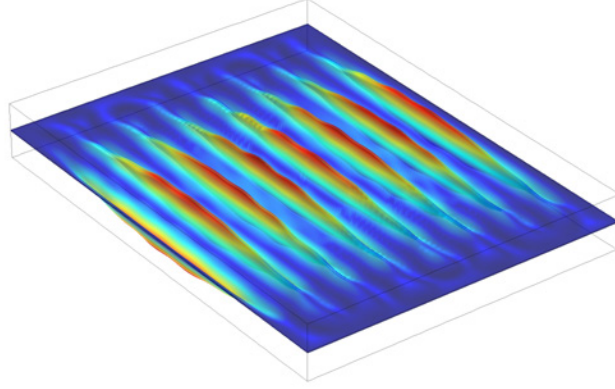


Figure 3.4: Panel response from excitation with a plane wave at $f = 6,800\text{Hz}$

3.4.1 Theory for the Natural Frequencies of a Rectangular Plate

A modal analysis allows for the solution of the natural frequencies, or eigenfrequencies, and the corresponding mode shapes of a solid structure. A panel oscillates at its natural frequency once it is set in motion, i.e., acted upon by an external force. For a flat plate, the transverse displacement is given by the differential equation from Kirchhoff's plate theory,

$$D\nabla^4 w(x, y, t) + \gamma \frac{\partial^2 w(x, y, t)}{\partial t^2} = 0, \quad 0 \leq x \leq a, 0 \leq y \leq b \quad (3.1)$$

where the two-dimensional biharmonic operator, ∇^4 , in Cartesian coordinates, is

$$\nabla^4 = \frac{\partial^4}{\partial x^4} + 2 \frac{\partial^2}{\partial x^2} \frac{\partial^2}{\partial y^2} + \frac{\partial^4}{\partial y^4} \quad (3.2)$$

The mass per unit area, γ , is calculated as,

$$\gamma = \rho h \quad (3.3)$$

where ρ is the density of plate in [grams/m³], and h is the thickness of the solid plate in [m]. The flexural rigidity, or bending stiffness, D , is then calculated with

$$D = \frac{Eh^3}{12 \cdot (1 - \nu^2)} \quad (3.4)$$

where E is Young's modulus in [GPa] and ν is Poisson's ratio. Separation of variables is used to determine the transverse displacement of the plate, w , as

$$w(x, y, t) = W(x, y) \cos(\omega t + \theta) \quad (3.5)$$

where $W(x, y, t)$ is the eigenfunction. Substitution of Equation 3.5 into Equation 3.1 produces an eigenvalue problem,

$$\left(\frac{\partial^4}{\partial x^4} + 2 \frac{\partial^2}{\partial x^2} \frac{\partial^2}{\partial y^2} + \frac{\partial^4}{\partial y^4} \right) W(x, y) - \frac{\gamma \omega^2}{D} W(x, y) = 0 \quad (3.6)$$

where ω is the angular frequency, or radian frequency, in [rad/s]. The mode shape, $W(x, y)$, of the simply supported plate is then,

$$W(x, y) = Q \sin \frac{i\pi x}{a} \sin \frac{j\pi y}{b} \quad (3.7)$$

where i and j are mathematical indicies. Substitution of Equation 3.7 into Equation 3.6 with the following boundary conditions,

$$w = 0, \frac{\partial^2 w}{\partial x^2} = 0 \text{ at } x = 0 \text{ or } x = a \quad (3.8)$$

$$w = 0, \frac{\partial^2 w}{\partial y^2} = 0 \text{ at } y = 0 \text{ or } y = b \quad (3.9)$$

yields the characteristic equation

$$\pi^4 \left(\frac{i^2}{a^2} + \frac{j^2}{b^2} \right)^2 - \frac{\gamma \omega^2}{D} = 0, i, j = 1, 2, \dots \quad (3.10)$$

The radian frequency of the plate, the roots of Equation 3.10, is Equation 3.11,

$$\omega_{ij}(i, j) = \pi^2 \left[\left(\frac{i}{a} \right)^2 + \left(\frac{j}{b} \right)^2 \right] \cdot \sqrt{\frac{D}{\gamma}} \quad (3.11)$$

The natural frequencies of the plate are then found as,

$$f_{ij} = \frac{\omega_{ij}(i, j)}{2\pi} \quad (3.12)$$

and they have units of [Hz], or, cycles per second. The equations above are found, in various formats, in several texts about vibrations [40] [41] [42] [43].

3.4.2 Theory for Transmission Loss through a Rectangular Plate

A pressure wave that impacts a structure at normal incidence is defined as a planar acoustic wave, and is given by

$$\mathbf{p}_i(x, y, z, t) = \mathbf{P}_i(x, y)e^{j(\omega t - k_1 z)} \quad (3.13)$$

where $\mathbf{p}_i(x, y, z, t)$ is the incident pressure in [dB], $\mathbf{P}_i(x, y)$ is the complex amplitude of an incident pressure wave, $j = \sqrt{-1}$, ω is the angular frequency in [rad/s], k is the wave number, and z is the coordinate normal to the plane of the panel. At steady state, the pressure reflected and transmitted are

$$\mathbf{p}_r(x, y, z, t) = \mathbf{P}_r(x, y)e^{j(\omega t + k_1 z)} \quad (3.14)$$

$$\mathbf{p}_t(x, y, z, t) = \mathbf{P}_t(x, y)e^{j(\omega t - k_2 z)}. \quad (3.15)$$

The wave numbers, k_1 and k_2 are defined as

$$k_1 = \frac{\omega}{c_1} \quad (3.16)$$

$$k_2 = \frac{\omega}{c_2} \quad (3.17)$$

where c_1 and c_2 are the speeds of sound in [m/s]. The pressure transmission coefficient is defined as

$$\mathbf{T} = \frac{\mathbf{P}_t}{\mathbf{P}_i}. \quad (3.18)$$

In the case of a periodic plane wave, the intensity transmission coefficient is real, as

$$T_I = \frac{I_T}{I_I} = \left(\frac{r_1}{r_2} \right) \|\mathbf{T}\|^2 \quad (3.19)$$

where I_T is the transmitted intensity, I_I is the incident intensity, and r is the characteristic acoustic impedance, such that

$$r_1 = \rho_1 c_1 \quad (3.20)$$

$$r_2 = \rho_2 c_2. \quad (3.21)$$

In the case of three layers, air, aluminum, then air, for instance, the equations above can be used to derive the intensity transmission coefficient for a panel. It is found by assuming continuity of the normal specific acoustic impedance at the media boundaries and that the incident and transmitted cross sectional area of the sound beam is the same. From the theory in Kinsler, et al [44], and some algebraic manipulation, the intensity transmission coefficient is found as

$$T_I = \frac{4}{2 + (r_3/r_1 + r_1/r_3) \cos^2 k_2 h_2 + (r_2^2/r_1 r_3 + r_1 r_3/r_2^2) \sin^2 k_2 h_2}. \quad (3.22)$$

Since the aluminum has a higher impedance than the surrounding air domains, $r_2 \gg r_1, r_3$ the intensity transmission coefficient can be reduced to

$$T_I = \frac{1}{1 + \frac{1}{4} (r_2/r_1)^2 \sin^2 k_2 h_2}. \quad (3.23)$$

The sound transmission loss is shown in as,

$$TL = 10 \log_{10} \frac{1}{T_I} = 10 \log_{10} \frac{\Pi_I}{\Pi_T} = 10 \log_{10} \left(\frac{|p_i|^2}{|p_t|^2} \right) \quad (3.24)$$

where Π_T is the transmitted sound power, and Π_I is the incident sound power [45].

3.5 Acoustic Transmission through a Sandwich Panel

Figure 3.5, a graphical representation of an acoustic plane wave impinging, at normal incidence, upon an offset-core honeycomb sandwich panel, is annotated with the incident wave, p_i , the reflected wave, p_r , and the transmitted wave, p_t . The air domains, the first honeycomb core, and the offset honeycomb core are labeled as 1, 2, 3, and 4, respectively.

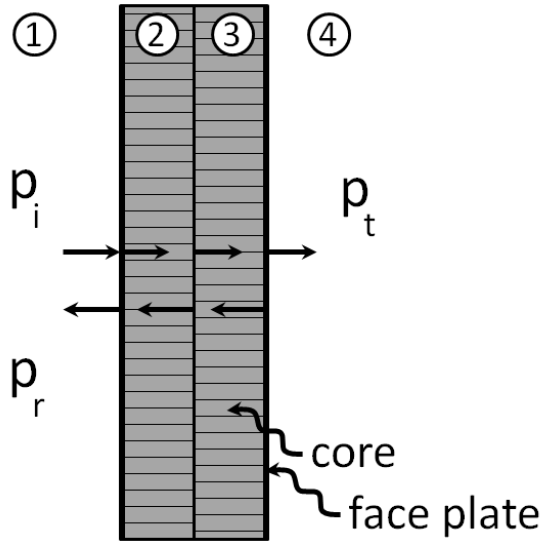


Figure 3.5: A graphical representation of an acoustic wave impinging upon an offset-core honeycomb panel at normal incidence

3.6 Finite Element Analysis of Honeycomb Sandwich Panels

In many works, authors do not explicitly model the honeycomb core, as the computational expense increases dramatically as the number of cells in the honeycomb core increases. Often, the cores are replaced by an equivalent continuum model, and consideration is not given to the cellular structure of the core material [46]. In a continuum model, the core structure is reduced to a series of effective properties [47]. Typically, the face plates are modeled as shells, and the honeycomb cores are modeled as orthotropic materials [25]. In many cases, using a panel's effective properties rather than its actual geometry is the most efficient method for conducting FEA, but in cases where local stress distribution within the core and face plate material must be determined, a continuum model will not suffice [48]. In recent years, some authors have modeled the actual geometry of the core with various FEA programs [38] [49]. In the current study, the geometry of one honeycomb core is being offset with a secondary honeycomb core, so a continuum model would seemingly not produce a sufficient description of the acoustic wave passing through the honeycomb structure.

For the models of offset-core honeycomb sandwich panels, there are several ways that the core layers could be offset from one another [2]. In a simple case, for instance, one honeycomb could be moved half the length of a cell in the horizontal direction or in the vertical direction. For this study, only the vertical offset direction was studied. So that the vertical offset is clear to the reader, an image of a single-core honeycomb sandwich panel is shown in Figure 3.6, and, in comparison, a transparent

image of an offset-core honeycomb panel is shown in Figure 3.7. In, Figure 3.7, the first core is shown in black, and the core that is offset is shown in blue.

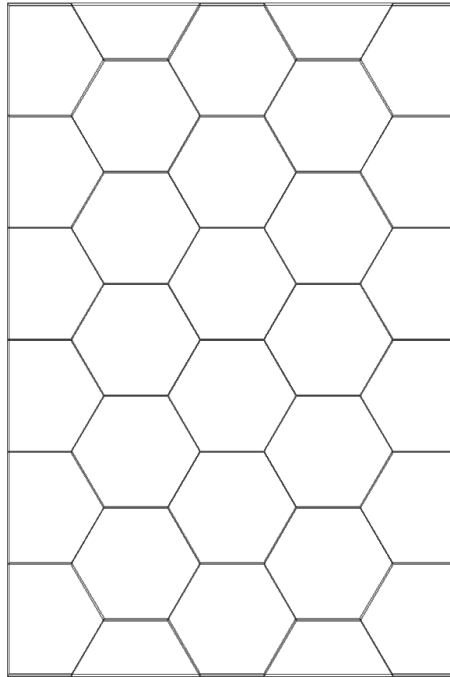


Figure 3.6: A transparent view of a single-core honeycomb panel

The face plate thickness, t_f , is chosen to be 0.02 in., and the core thicknesses, h_c , is chosen to be 0.250 in. The distance between walls in core cells, S , was given a bit of variation, as 0.990 in., 0.740 in., and 0.490 in., were used for 2 in. x 3 in. panels so the results could be compared for scaling cell size. These distances, along with the cell wall thickness, t_c , of 0.005 in., would allow for total cell sizes, S_T , of 1 in., 0.75 in., and 0.5 in. Similar sizes are commonly sold by manufacturers Goodfellow and Hexcel.

For scaling the panel size from 2 in. x 3 in. to 4 in. x 6 in., and finally to 8 in. x 12 in., only the 1 in. cell size was used so that the computational expense

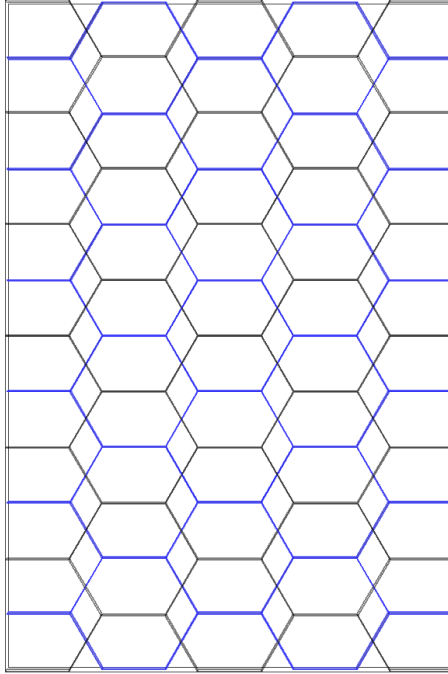


Figure 3.7: A transparent view of a offset-core honeycomb panel in which the core layers are vertically offset

would not become prohibitive during the natural frequency study. A summary of the geometries for single-core honeycomb panels, as described above, is shown in Table 3.1. A summary of the geometries that are studied for offset-core honeycomb panels is shown in Table 3.2. Only the 2 in. x 3 in. panels are explored, however, for the transmission loss study.

Table 3.1: Single-core Panel Geometries

Panel Length [in]	Panel Width [in]	Panel Thickness [in]	Cell Size [in]
a	b	h	S_T
2	3	0.29	0.50
2	3	0.29	0.75
2	3	0.29	1.00
4	6	0.29	1.00
8	12	0.29	1.00

Table 3.2: Offset-core Panel Geometries

Panel Length [in]	Panel Width [in]	Panel Thickness [in]	Cell Size [in]
a	b	h	S_T
2	3	0.54	0.50
2	3	0.54	0.75
2	3	0.54	1.00
4	6	0.54	1.00
8	12	0.54	1.00

3.6.1 Modal Analysis

In this model, the first twenty-four natural frequencies of the honeycomb sandwich panels are computed using the structural mechanics module within COMSOL Multiphysics. Damping was not included in the eigenfrequency analysis. Secondly, the adhesive layer that is typically used to attach the face plates to the honeycomb core was not considered in the model. For cases where the adhesive layer is below 1 mm thickness, it is a reasonable assumption that the eigenfrequency of the hon-

eycomb sandwich panel is not significantly affected by the adhesive layer [50]. The eigenvibration properties do, however, significantly depend on the geometries of the honeycomb cell size, core thickness, and face plate thickness. For these reasons, the adhesive layer is neglected. The face plates are assumed to have an equal thickness, t_f . For simplicity, it is assumed that the honeycomb sandwich panels are shear resistant, i.e., there is no sliding between the layers of the panel.

After computing the eigenfrequencies of the honeycomb sandwich panels, a 1 Newton impulse force was applied normal to the face plate boundary. To do this, a smoothed rectangular function was multiplied times the force that strikes the boundary. Since the function is applied in this manner, it acts as an impulse on the panel. The total displacement of a point near the center of the panel as a function of frequency can then be plotted to show the response of the system, and the fundamental frequencies, along with various resonances, should appear as spikes on the plot.

3.6.2 Transmission Loss

In this model, air domains are separated by the honeycomb sandwich panel, a solid elastic structure. An acoustic pressure wave impacts the structure with the consequence of a reflected wave and a wave transmitted, with an intensity loss, through the structure. This TL through the structure is found, as a function of frequency, for each sandwich panel size and geometry. The acoustic-structure interaction module was primarily used to obtain the transmission loss through the honeycomb panels. Due to high computational expense, only the 2in. x 3in. panels were analyzed in the transmission loss study.

To describe an acoustic field in the classical sense, flow is assumed to be lossless, adiabatic, and viscous effects are neglected [51]. The wave equation governs the behavior of the field, as

$$\frac{1}{\rho c^2} \frac{\partial^2 p}{\partial t^2} + \nabla \cdot \left(-\frac{1}{\rho} \nabla p + \mathbf{q}_d \right) = \mathbf{Q}_m. \quad (3.25)$$

where t is time, c is the speed of sound, ρ is the density of the fluid, p is pressure, \mathbf{q}_d is the dipole source term, and \mathbf{Q}_m is the monopole source term. A general way to express the pressure term, p , is

$$p = p(\hat{\mathbf{x}}) e^{i\omega t}. \quad (3.26)$$

Using this harmonic pressure term, the wave equation can then be reduced as

$$\nabla \cdot \left(-\frac{1}{\rho} \nabla p + \mathbf{q}_d \right) - \frac{k^2 p}{\rho} = \mathbf{Q}_m \quad (3.27)$$

This is the Helmholtz equation. The pressure acoustics feature within COMSOL Multiphysics' acoustic-structure interaction module allows for solutions to the Helmholtz equation for sound pressure. By setting the source terms, \mathbf{q}_d and \mathbf{Q}_m to a value of 0, the the plane wave solution to the Helmholtz equation emerges such that

$$p = P e^{i(\omega t - \mathbf{k} \cdot \hat{\mathbf{x}})} \quad (3.28)$$

where P is the wave amplitude, \mathbf{x} is the direction, ω is the angular frequency, and \mathbf{k} is the wave number. The sound pressure level is then found with

$$L_p = 20 \log \left(\frac{p_{rms}}{p_{ref}} \right) \quad (3.29)$$

where the root mean square pressure, p_{rms} , is

$$p_{rms} = \sqrt{\frac{1}{2}pp^*}. \quad (3.30)$$

p_{ref} is the reference pressure, and for air, it is 20 μ Pa. The * in Equation 3.30 denotes the complex conjugate. The overall sound pressure level can then be found as

$$L_T = 10 \log \left(\sum 10^{L_p/10} \right). \quad (3.31)$$

3.6.3 Material Properties and Boundary Conditions

Only two materials were considered during development of the models. The honeycomb sandwich panels, the core and the face plates, were assumed to be a standard aluminum with a density, ρ , of 2700 kg/m³, a Young's modulus, E , of 70 GPa, a Poisson's ratio, ν , of 0.33, and a speed of sound, c , of 6420 m/s. Considering both the face plates and the core as the same material is done for simplicity for the FEA, as it is done in other works [36]. The honeycomb sandwich panels were clamped (fixed in x , y , and z directions) on blue highlighted boundaries of the two face plates, as shown in Figure 3.8 and Figure 3.9 in order to simulate typical experimental conditions in which the panel would be installed in a window between an anechoic chamber and a reverberation room. Even though the sides of the face plates cannot

move in the x , y , or z direction, the core is not fixed at the sides. This was done for both single-core and offset-core honeycomb panels. Clamped edge conditions are expected to increase the stiffness of the panel, and produce natural frequencies higher than what would be expected of those with a free edge conditions [37].

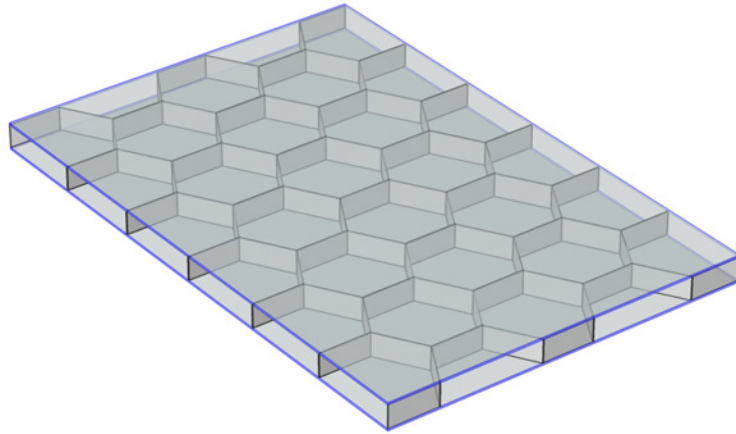


Figure 3.8: Fixed boundaries of a single-core honeycomb panel

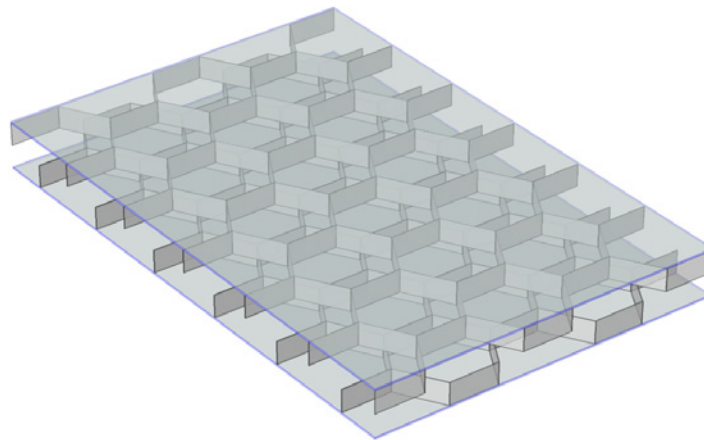


Figure 3.9: Fixed boundaries of an offset-core honeycomb panel

In the transmission study, the honeycomb panels were sandwiched between air domains, and the cellular structure of the honeycomb was filled with air. Dry air domains at exterior of the plates and within the cells have a density, ρ , at standard temperature and pressure (20 °C and 101.325 kPa) of 1.2754 kg/m³ and a speed of sound, c , of 343.2 m/s. Once again, the panels were fixed along sides as shown above. A plane wave with a pressure amplitude of 20 Pa (120 dB SPL) radiates from the topmost boundary as with the benchmark problem. The boundaries surrounding the plate are set to the impedance value for air, a r_{air} of 411.6 Pa·s/m.

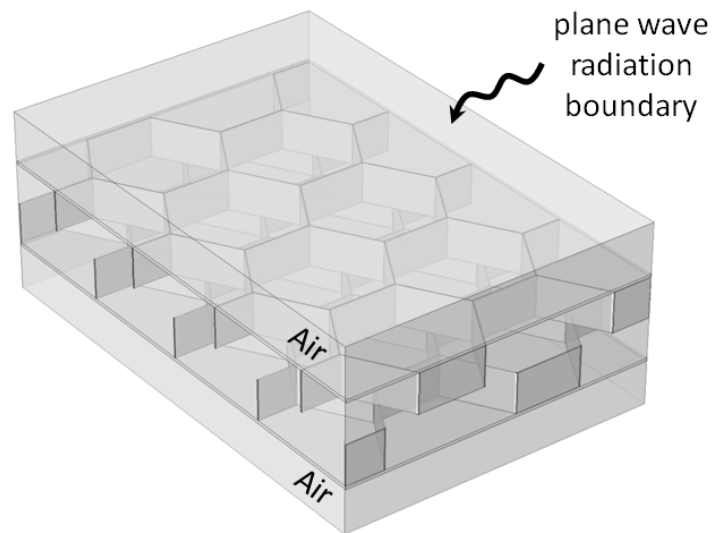


Figure 3.10: Plane wave radiation toward offset-core honeycomb panel

The boundary conditions that can be used within COMSOL Multiphysics are shown in the COMSOL Multiphysics manual [51]. In COMSOL Multiphysics, the plane wave radiation boundary condition is given as

$$-\mathbf{n} \cdot \left(-\frac{1}{\rho} (\nabla p_{tot} - \mathbf{q}_d) \right) + i \frac{kp}{\rho} + i \frac{\Delta_T p}{2k\rho} = Q_i \quad (3.32)$$

The monopole source term, Q_i is

$$Q_i = i \frac{k}{\rho} p_i + i \frac{\Delta_T p_i}{2k\rho} + \mathbf{n} \cdot \frac{1}{\rho} \nabla p_i. \quad (3.33)$$

where Δ_T at a point on the boundary is the Laplace operator in the tangent plane at that point. As stated previously, in the case of a plane wave, however, the source terms, \mathbf{q}_d and \mathbf{Q}_m are zero. p_{tot} is the total pressure field, and it is given as

$$p_{tot} = p_b + p_s \quad (3.34)$$

where p_b is the background pressure field, and p_s is the scattered pressure field. The incident pressure field term in Equation 3.33 is

$$p_i = p_0 e^{-ik \left(\frac{\mathbf{r} \cdot \mathbf{e}_k}{\|\mathbf{e}_k\|} \right)} \quad (3.35)$$

where p_0 is the wave amplitude, \mathbf{k} is the wave vector, \mathbf{e}_k is the direction vector, and \mathbf{r} is the location on the boundary. The acoustic-structure interaction module in COMSOL Multiphysics sets the boundary load, F in [force/unit area], on the panel as

$$\mathbf{F} = -\mathbf{n}_s p. \quad (3.36)$$

\mathbf{n}_s is given as the outward-pointing unit normal vector of the solid. As the panel is impacted by boundary load, F , it displaces. The normal acceleration of the solid then imposes an equal normal acceleration, a_n , on the fluid in the acoustics domain. This is,

$$-\mathbf{n}_a \cdot \left(-\frac{1}{\rho} \nabla p + \mathbf{q} \right) = a_n \quad (3.37)$$

where \mathbf{n}_a is the outward-pointing unit normal vector of the fluid. a_n is

$$a_n = (n_a \cdot \mathbf{u}) \omega^2 \quad (3.38)$$

where \mathbf{u} is the displacement vector of the solid structure. The impedance boundary condition is given as

$$-\mathbf{n} \cdot \left(-\frac{1}{\rho} (\nabla p_t - \mathbf{q}_d) \right) = -p_t \frac{i\omega}{r_i} \quad (3.39)$$

where the impedance, r_i , is set to the impedance of air. The fixed boundary condition that is used on the panel's sides is given as

$$\mathbf{u} = 0 \quad (3.40)$$

3.6.4 Mesh

A physics-driven free tetrahedral meshing sequence was used for the honeycomb sandwich panels. Finer meshes were applied to each model until convergence

was successful and the results were consistent with the previous coarser mesh. An example of the physics-driven, free tetrahedral mesh as applied to a 2in. x 3in. offset-core honeycomb sandwich panel is shown in Figure 3.11. A detailed view of the meshing at one corner of the panel is shown in Figure 3.12. In the transmission loss studies, air domains were also meshed. The meshing used for the transmission loss studies is shown in Figure 3.13.

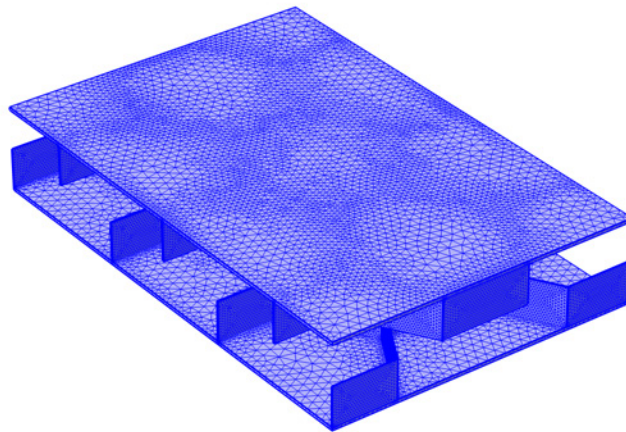


Figure 3.11: Physics-driven free tetrahedral mesh applied to an offset-core honeycomb sandwich panel

Low mesh resolution errors were avoided by consistently applying a "normal" or "fine" element size. For instance, for a 4in. x 6in. offset-core honeycomb sandwich panel, a predefined "fine" element size has a maximum element size of 0.48in., a minimum element size of 0.06in., a maximum element growth rate set to 1.45, a

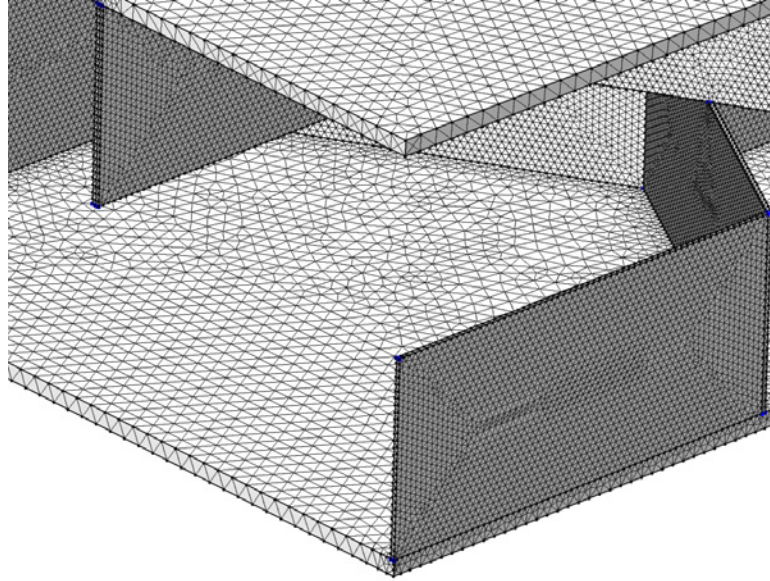


Figure 3.12: Detail view of a free tetrahedral mesh applied to an offset-core honeycomb sandwich panel

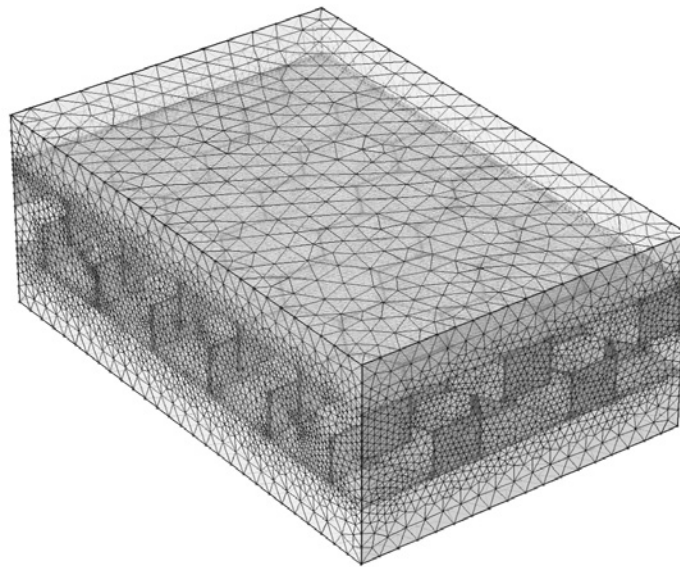


Figure 3.13: Free tetrahedral meshing of air domains and honeycomb panel for transmission loss studies

resolution of curvature set to 0.5, and a resolution of narrow regions set to 0.6. For comparison, a predefined "normal" element size for this structure has a maximum element size of 0.6in., a minimum element size of 0.108in., a maximum element growth rate set to 1.5, a resolution of curvature set to 0.6, and a resolution of narrow regions set to 0.5. An example of the mesh parameter setup is shown in Figure 3.14.

The screenshot shows the 'Element Size' configuration window in COMSOL. It includes a 'Calibrate for' dropdown menu set to 'General physics'. Below this, there are two radio buttons: 'Predefined' (which is selected) and 'Custom'. Next to the 'Predefined' button is another dropdown menu set to 'Fine'. A section titled 'Element Size Parameters' is expanded, revealing several input fields: 'Maximum element size' (0.48 in), 'Minimum element size' (0.06 in), 'Maximum element growth rate' (1.45), 'Resolution of curvature' (0.5), and 'Resolution of narrow regions' (0.6).

Figure 3.14: Mesh parameter setup within the COMSOL Multiphysics environment

The types and number of mesh elements that were used in each study is summarized in Table 3.3 and Table 3.4.

The COMSOL Multiphysics manual indicates that at least five domain elements per wavelength are needed to ensure that a mesh is dense enough for a solution to converge [51]. This was considered when developing the mesh for the transmission study, and sufficient meshes were applied.

Table 3.3: Mesh Elements for Each Natural Frequency Study

a [in]	b [in]	S_T [in]	Type Core	Element Vertex	Element Edge	Element Boundary	Element Domain
2	3	1	SCHP	156	4,228	83,000	129,624
2	3	1	OCHP	344	7,414	109,160	169,729
2	3	0.75	SCHP	266	5,905	96,291	152,053
2	3	0.75	OCHP	616	10,927	134,900	210,134
2	3	0.50	SCHP	556	9,301	119,039	190,644
2	3	0.50	OCHP	1,302	17,975	179,465	282,965
4	6	1	SCHP	484	16,457	453,898	707,878
4	6	1	OCHP	1,152	30,792	601,470	939,208
8	12	1	SCHP	2,122	34,871	294,511	290,489
8	12	1	OCHP	2,954	51,195	506,583	1,119,548

Table 3.4: Mesh Elements for Each Transmission Loss Study

a [in]	b [in]	S_T [in]	Type Core	Element Vertex	Element Edge	Element Boundary	Element Domain
2	3	1	SCHP	164	4,449	90,922	562,598
2	3	1	OCHP	396	8,608	130,393	775,944
2	3	0.75	SCHP	274	6,121	103,417	610,155
2	3	0.75	OCHP	624	11,165	144,242	909,293
2	3	0.50	SCHP	564	9,541	126,700	694,467
2	3	0.50	OCHP	1,310	18,258	190,415	1,132,539

3.6.5 Solver

For the modal analysis, a direct solver called multifrontal massively parallel sparse direct solver (MUMPS), was used.

For the transmission loss analysis, the iterative method multigrid was used. The generalized minimal residual method (GMRES) and the flexible generalized minimal residual method (FGMRES) are used as the linear system solvers, and geometric multigrid is used as a preconditioner. COMSOL Multiphysics defaults the preconditioner to the incomplete LU, but for more complex, 3D acoustic problems, it should be switched to multigrid [51]. Within the presmoothing and postsmoothing options, Krylov preconditioner was selected with GMRES selected as the solver. An abundance of information about multigrid solvers, GMRES, FGMRES, and Krylov preconditioning can be found in the COMSOL Reference Manual [51].

CHAPTER 4

RESULTS AND DISCUSSION

4.1 Benchmarking Results

4.1.1 Results of Modal Analysis

The natural frequencies, $f(i,j)$, were determined for $f(1,1)$, $f(1,2)$... $f(6,6)$. The results from theory and from the FEA analysis, along with the Matlab code for the calculations, are shown in Appendix A. Specifically, the results from theory are shown in Table A.1, and the results from FEA are shown in Table A.2. Displacement field plots are shown, in Table A.4, to better visualize the eigenmodes of the rectangular plate. The displacement field plot for the $f(1,1)$ mode, or fundamental frequency, is also shown in Figure 4.1. A comparison of theory to FEA is shown in Figure 4.2. Figure 4.2 shows that the results from theory closely resemble the results from the FEA. The percentage error between the theory and FEA results is shown in Table A.3.

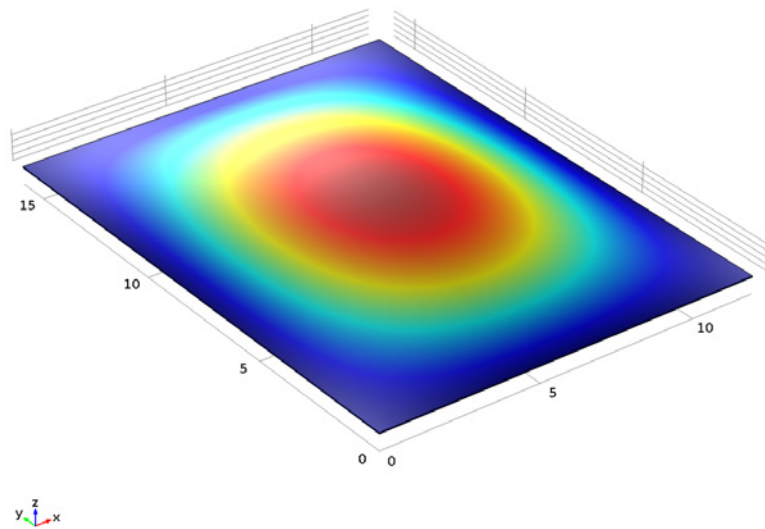


Figure 4.1: Displacement field plot for the fundamental mode of a rectangular plate ($f_n = 41.79\text{Hz}$)

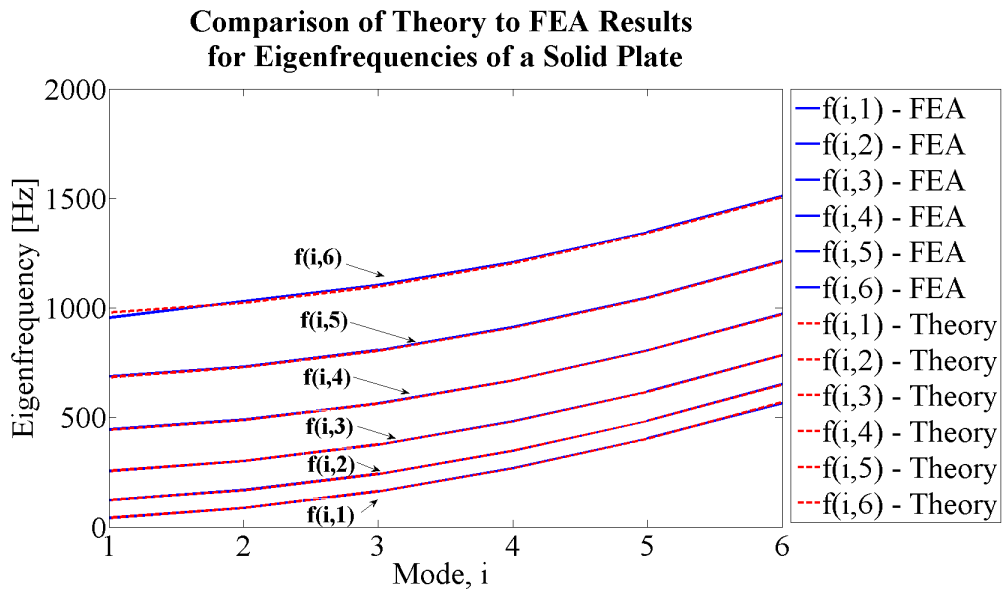


Figure 4.2: Comparison of theory to FEA results for the natural frequencies of a solid aluminum plate

4.1.2 Results of Acoustic Transmission Loss Study

The acoustic transmission loss of an aluminum plate was determined. The intensity transmission coefficient, T_I , obtained from theory and from the FEA, versus frequency for a 10kHz bandwidth, Δf , is plotted in Figure 4.3. A detailed view of Figure 4.3 is shown in Figure 4.4 for $f = 0\text{Hz}$ to 1kHz and in Figure 4.5 for $f = 1\text{kHz}$ to 10kHz . A similar trend is shown, as the FEA T_I begins to deviate slightly at some frequencies $> 2200\text{ kHz}$. However, the error is very low. This indicates that FEA is appropriate for approximating transmission loss across a panel, especially in the low to mid frequency range.

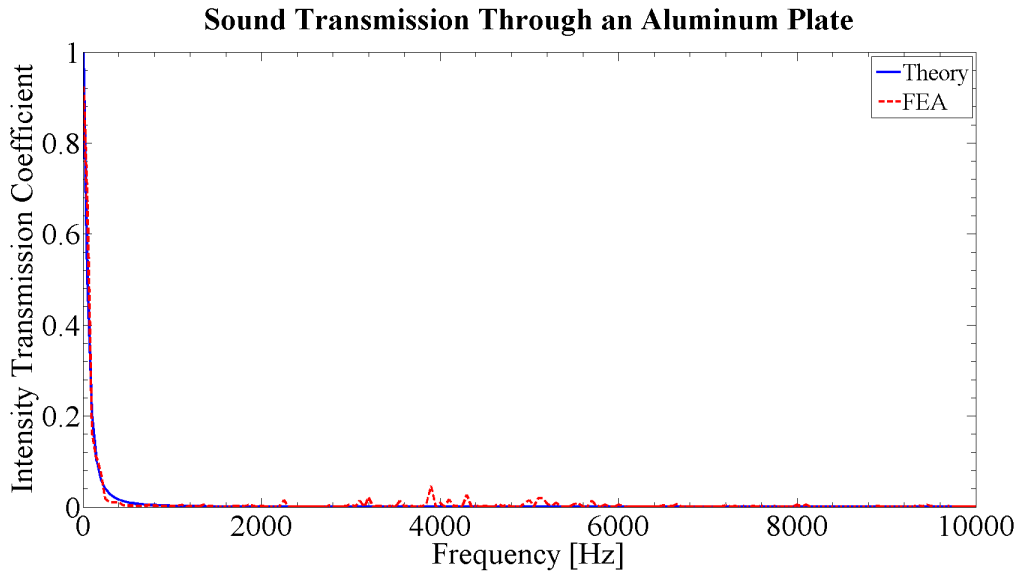


Figure 4.3: Comparison of theory to FEA results for the transmission loss through a solid aluminum plate

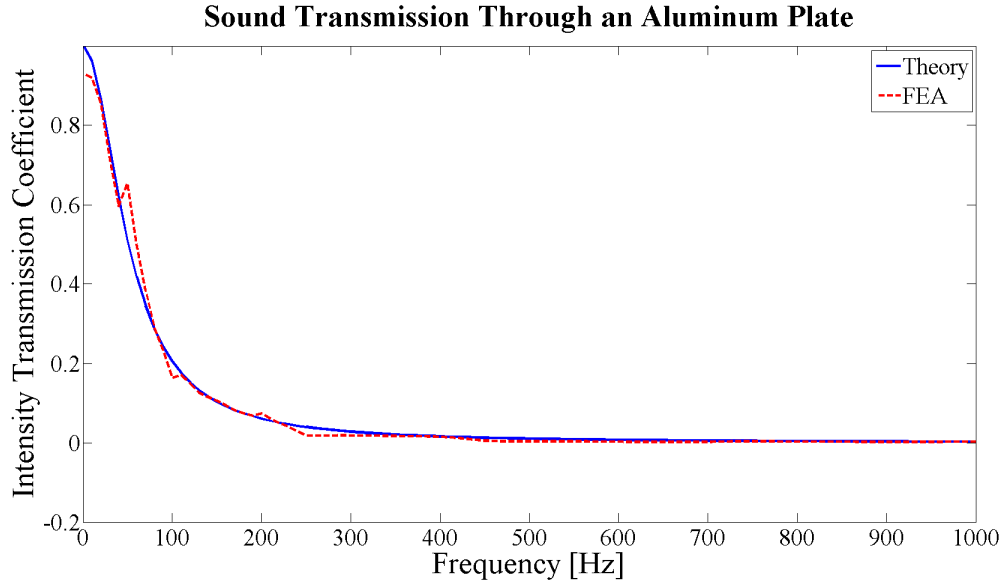


Figure 4.4: Detailed view of Figure 4.3 for $f = 0\text{Hz}$ to 1kHz

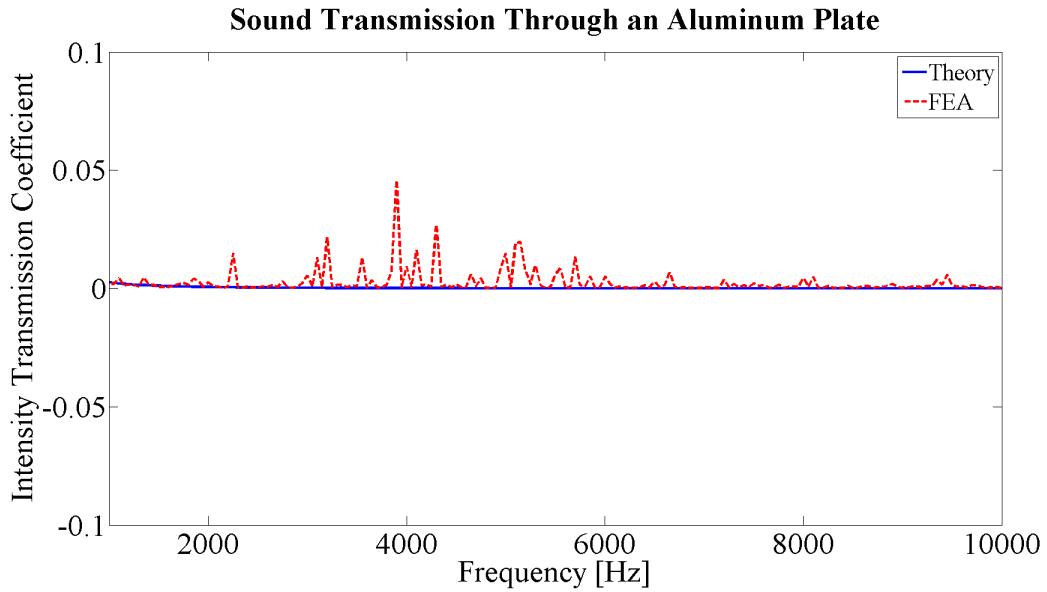


Figure 4.5: Detailed view of Figure 4.3 for $f = 1\text{kHz}$ to 10kHz

4.2 Modal Analysis of Honeycomb Panels

COMSOL Multiphysics was set to solve for the first 24 natural frequencies of the panels. The tabulated results are displayed in Appendix B.

4.2.1 Single-core Honeycomb Panel

The first twenty four natural frequencies of the single-core honeycomb panels are tabulated in Table B.2. The data in Table B.2 shows that the natural frequencies of a single-core honeycomb panel increases as the honeycomb cell size decreases. This is consistent with other numerical works [50]. It makes sense, since as the honeycomb cell size decreases, the weight of the entire panel increases, and the stiffness of the face plates also increases. This trend is consistent with other experimental findings [52] [53]. The fundamental frequency for each fixed single-core honeycomb panel is summarized in Table 4.1.

Table 4.1: Fundamental Frequencies of Single-core Honeycomb Panels

Panel Length [in]	Panel Width [in]	Cell Size [in]	Fundamental Frequency [Hz]
a	b	S_T	f_n
2	3	0.50	9629.91
2	3	0.75	7367.02
2	3	1.00	5399.92
4	6	1.00	3356.22
8	12	1.00	962.40

The response of the 2in. x 3in., the 4in. x 6in., and the 8in. x 12in. single-core honeycomb panels is shown in Figure 4.6 through Figure 4.10. A point at the topmost center of each panel was chosen for evaluation of the total displacement. The fundamental frequencies that were found using the eigenfrequency solver are apparent as the largest spike in the response plots.

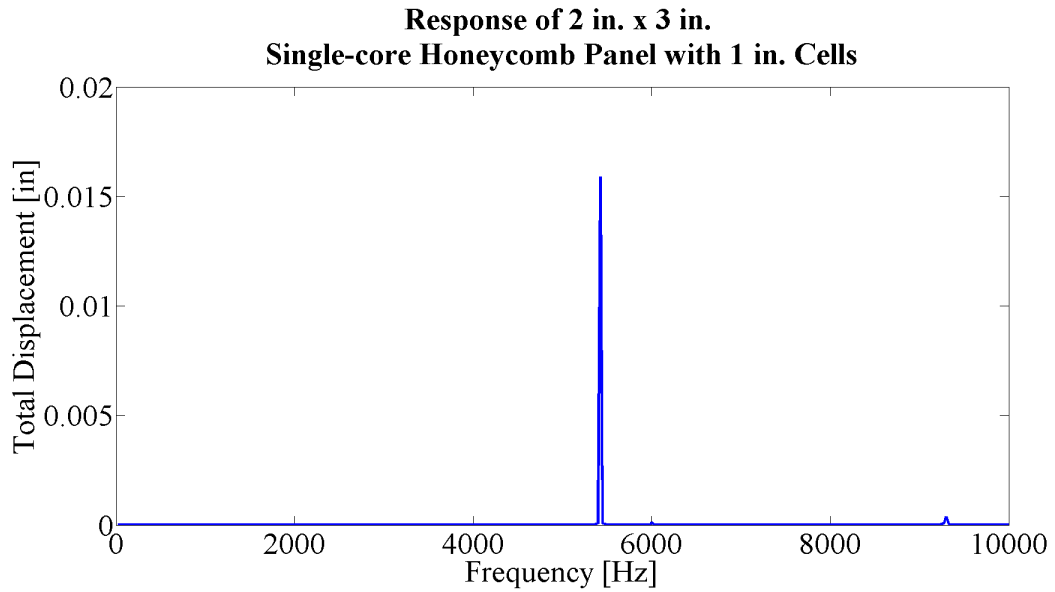


Figure 4.6: Response of a 2in. x 3in. single-core panel with 1in. cell size

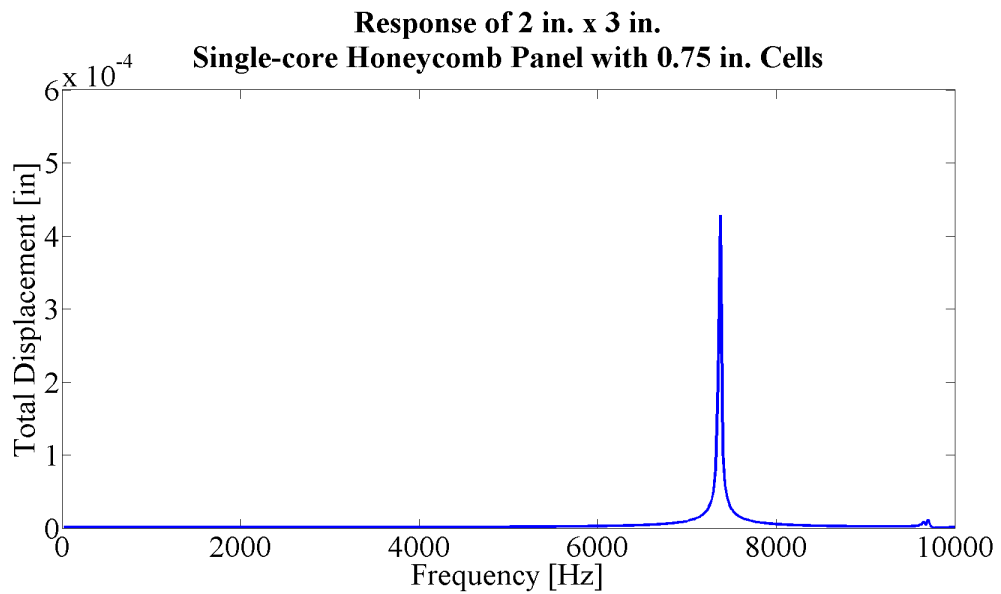


Figure 4.7: Response of a 2in. x 3in. single-core panel with 0.75in. cell size

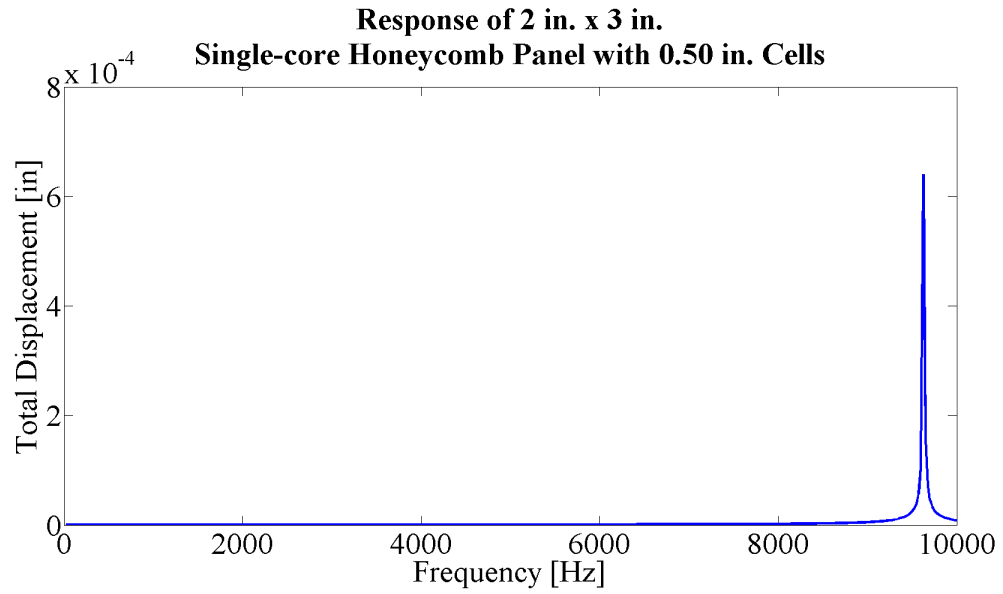


Figure 4.8: Response of a 2in. x 3in. single-core panel with 0.50in. cell size

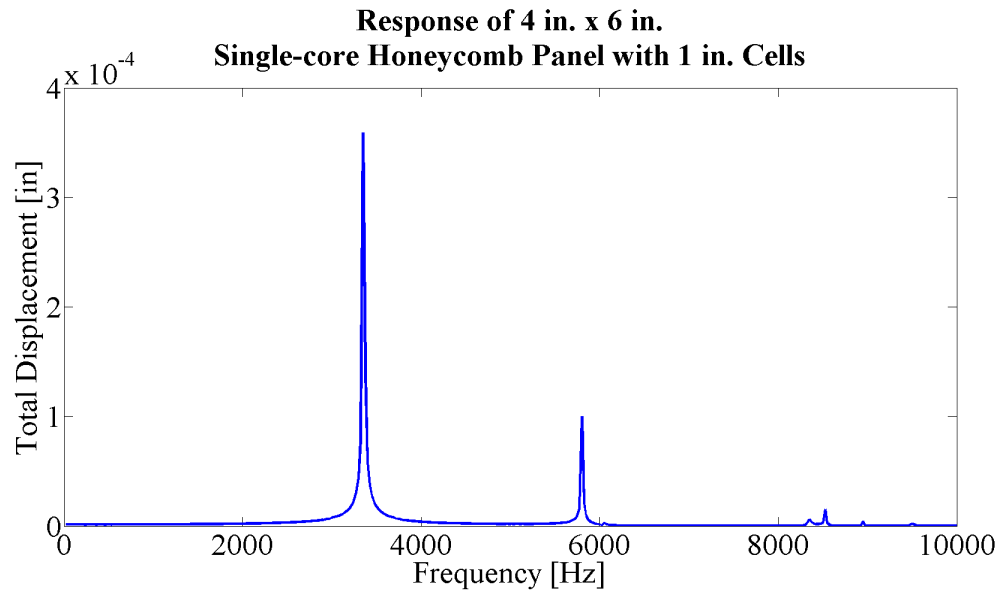


Figure 4.9: Response of a 4in. x 6in. single-core panel with 1in. cell size

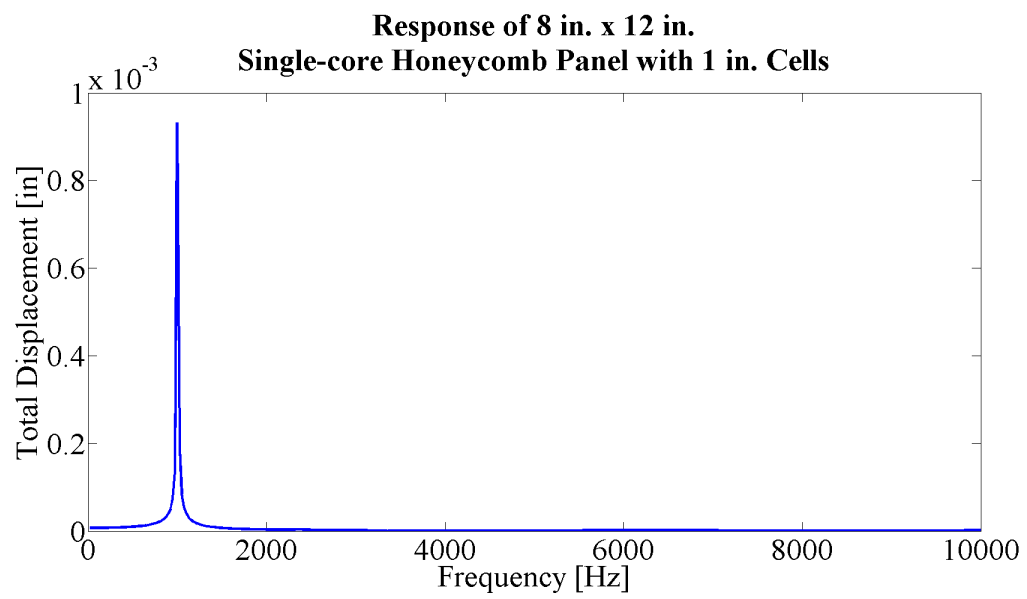


Figure 4.10: Response of a 8in. x 12in. single-core panel with 1in. cell size

4.2.2 Offset-core Honeycomb Panels

The increase in natural frequencies as the cell size decreases, a similiar trend that was shown for the single-core honeycomb panel, is also the case for the offset-core honeycomb panel. The first twenty four natural frequencies of offset-core honeycomb panels are shown in Table B.3. Including the secondary core and offseting it, however, produced a consistent reduction in eigenfrequencies for all three cell sizes. Once again, this is most likely due to the fact that the weight of the entire panel has increased. For visualization of the resultant mode shapes of the natural frequencies, a transparent image of a 4in. x 6in. offset-core panel with a 1in. cell size, displaying the (2,2) mode shape of the panel, is shown in Figure 4.11. This example shows exaggerated displacement, but it allows the reader to visualize how these types of panels would behave when vibrating. Images of other mode shapes for the 4in. x 6in. panel are given in Appendix B.

The fundamental frequency for each fixed offset-core honeycomb panel is summarized in Table 4.2.

Table 4.2: Fundamental Frequencies of Offset-core Honeycomb Panels

Panel Length [in]	Panel Width [in]	Cell Size [in]	Fundamental Frequency [Hz]
a	b	S_T	f_n
2	3	0.50	4481.53
2	3	0.75	3785.81
2	3	1.00	3363.37
4	6	1.00	1153.59
8	12	1.00	824.33

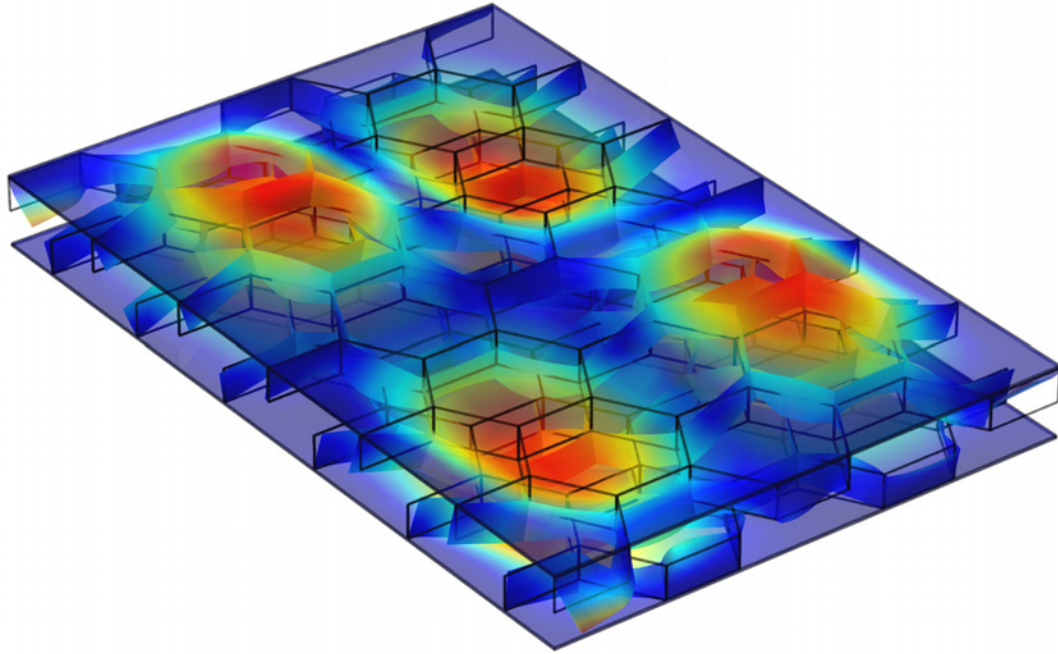


Figure 4.11: Mode shape of a 4in. x 6in. offset-core panel with 1in. cell size

The response of the 2in. x 3in., the 4in. x 6in., and the 8in. x 12in. offset-core honeycomb panels is shown in Figure 4.12 through Figure 4.16. A point at the topmost center of each panel was chosen for evaluation of the total displacement. The fundamental frequencies that were found using the eigenfrequency solver are, once again, easily recognized in these response plots as the largest spikes.

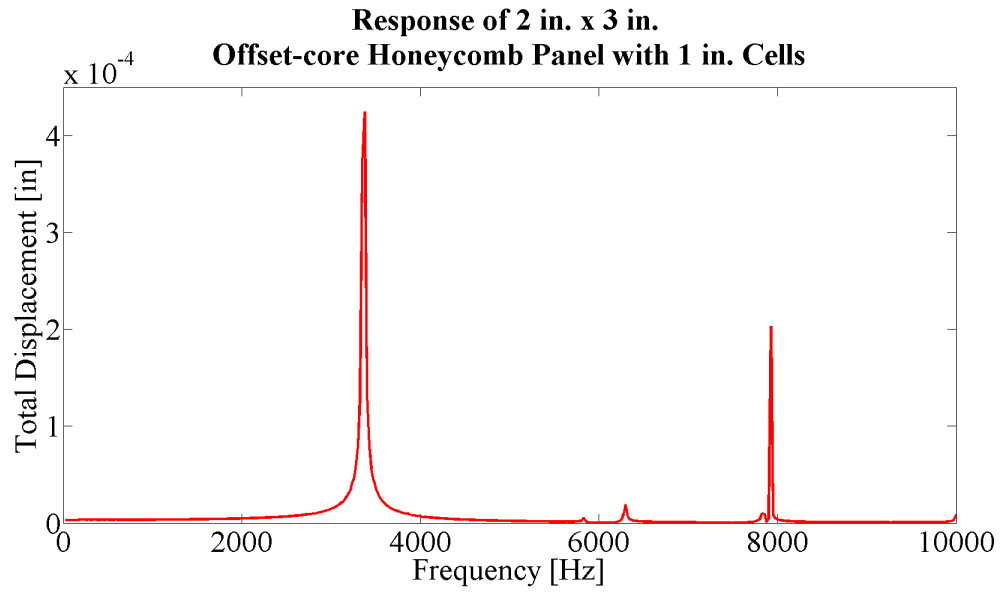


Figure 4.12: Response of a 2in. x 3in. offset-core panel with 1in. cell size

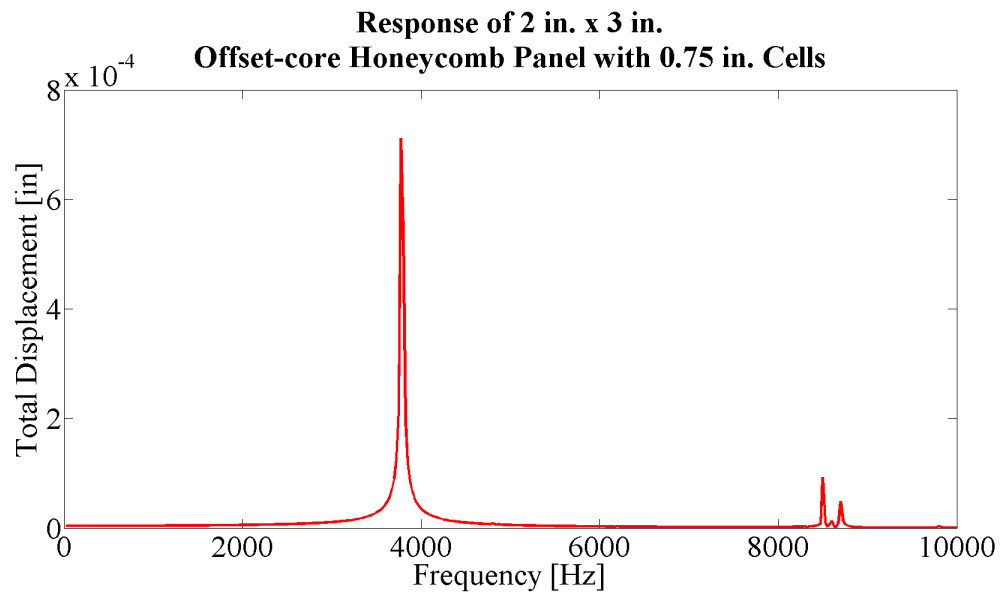


Figure 4.13: Response of a 2in. x 3in. offset-core panel with 0.75in. cell size

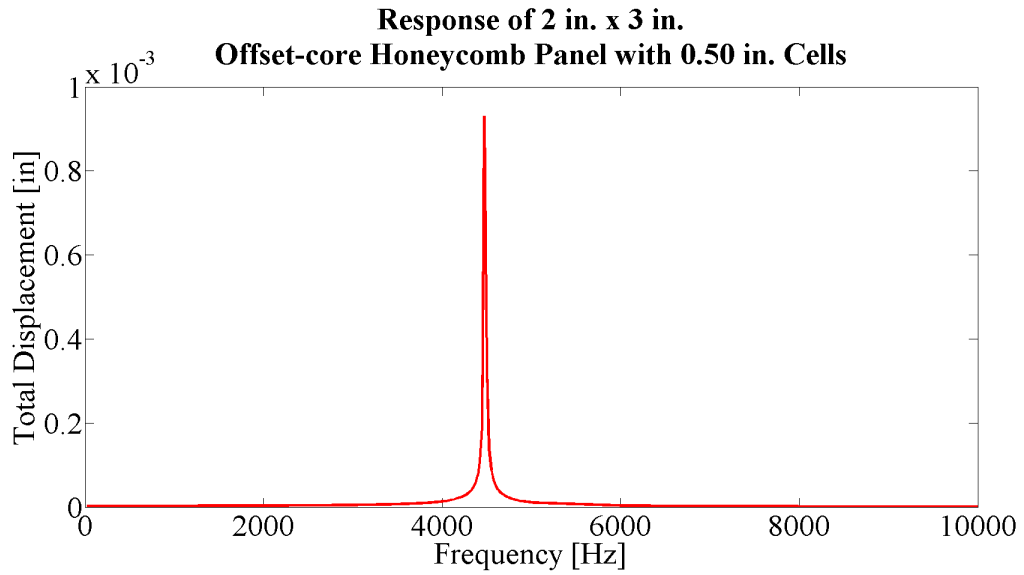


Figure 4.14: Response of a 2in. x 3in. offset-core panel with 0.50in. cell size

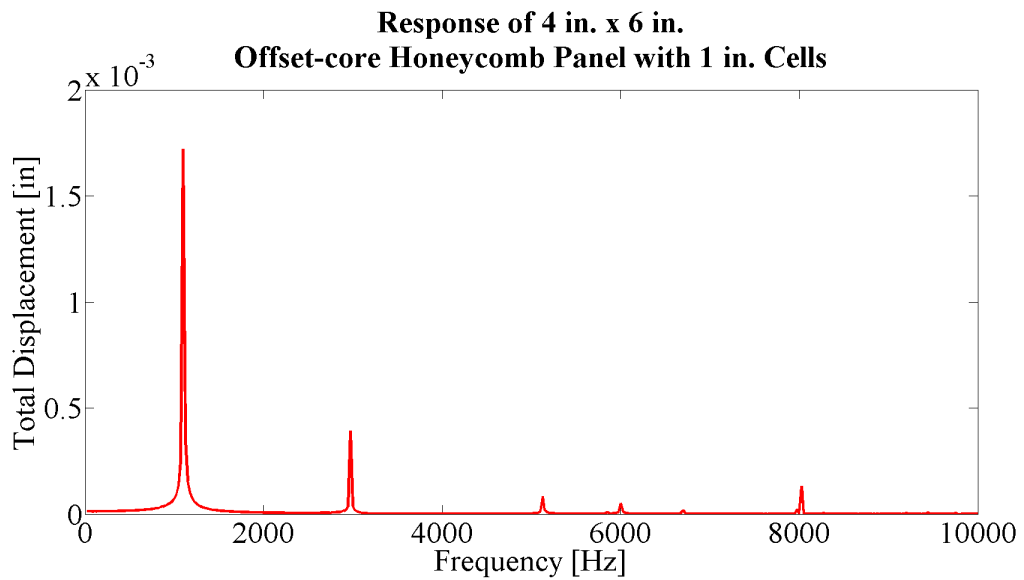


Figure 4.15: Response of a 4in. x 6in. offset-core panel with 1in. cell size

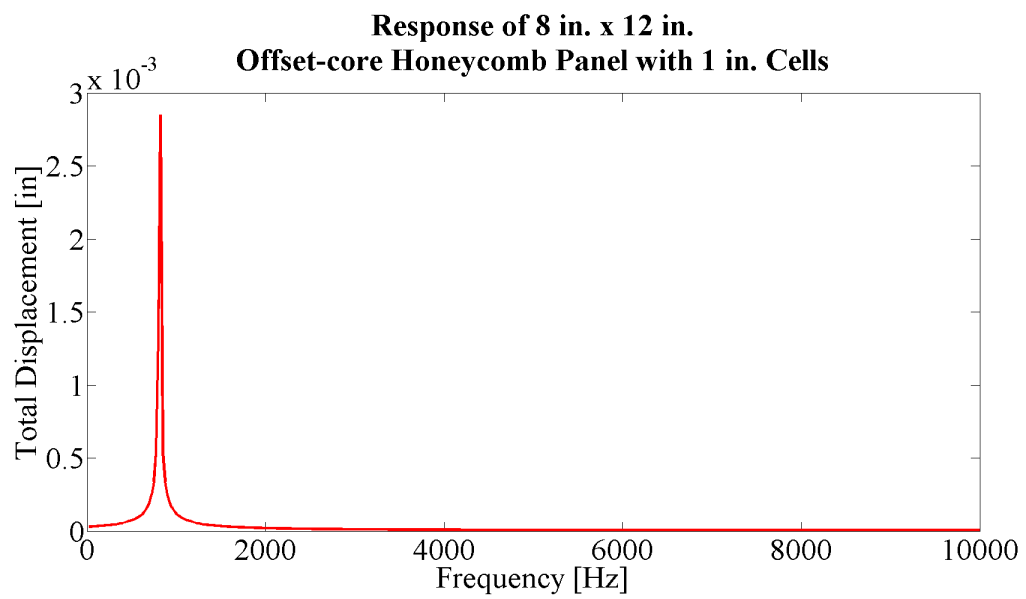


Figure 4.16: Response of a 8in. x 12in. offset-core panel with 1in. cell size

4.3 Transmission Loss of Honeycomb Panels

A surface average of the sound pressure level and the instantaneous intensity magnitude was taken on incident and transmitted sides of the panel. The incident and transmitted sound pressure levels for each panel are plotted in Figure 4.17 through Figure 4.22. The sound pressure levels for SChP and OChP for each cell size is then plotted in Figure 4.23 through Figure 4.25. Finally, the sound pressure levels are compared for the three SChP in Figure 4.26 and for the OChP in Figure 4.27.

The intensity magnitude was used to plot the transmission loss using Equation 3.24. The transmission loss is plotted, in Figure 4.28, Figure 4.29, and Figure 4.30 across the broadband frequency range of $\Delta f = 10,000\text{Hz}$ in steps of 50Hz for the 2in. x 3in. panel with 1in., 0.75in., and 0.50in. cell size, respectively. Finally, the transmission loss is compared for SChP in Figure 4.31 and for OChP in Figure 4.32.

The offset-core honeycomb panels perform better than the single-core honeycomb panels in the low-frequency range $< 1000\text{Hz}$. However, above the 1000Hz frequency, the single-core honeycomb panels tend to provide a consistent transmission loss across the band. There are some significant drops in transmission loss for the offset-core panels around the fundamental frequency of the panels. This drop indicates that the panel is, essentially, transparent to sound at that frequency. These minima shift higher into the broadband range as the cell size decreases, however, so it is possible that it could be mitigated with proper design. The three offset-core TL lines are plotted on the same graph as a comparison in Figure 4.32, and the shift is apparent. Even though it is noted that the single-core honeycomb TL is more

consistent across the band, for many frequencies the offset-core honeycomb panel has a TL that is higher by more more than 10dB. The transmitted overall sound pressure level (OASPL) for the 2in. x 3in. honeycomb panels is shown in Table 4.3.

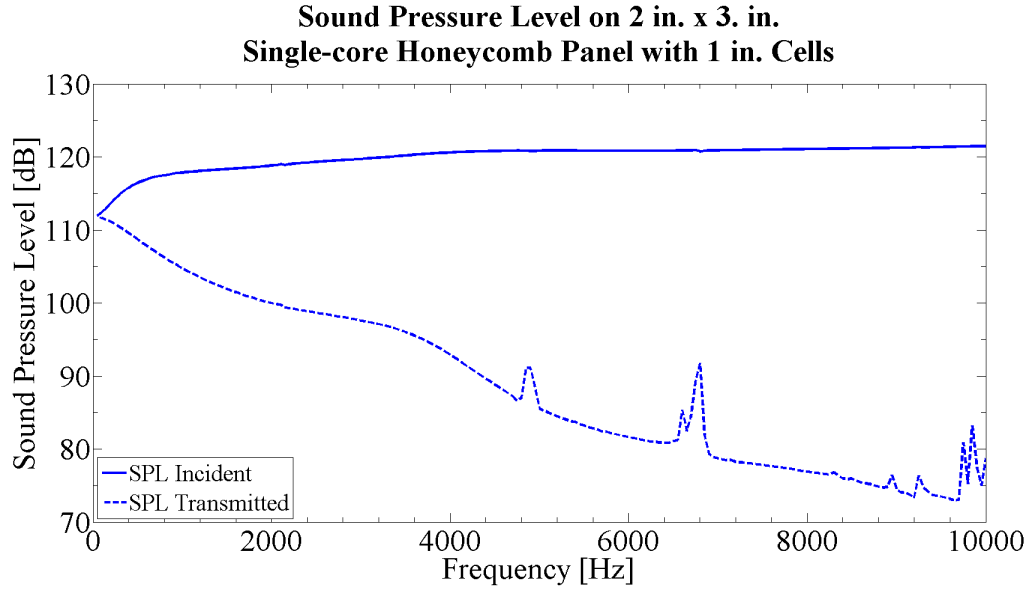


Figure 4.17: Sound pressure level on a 2in. x 3in. single-core panel with 1in. cell size

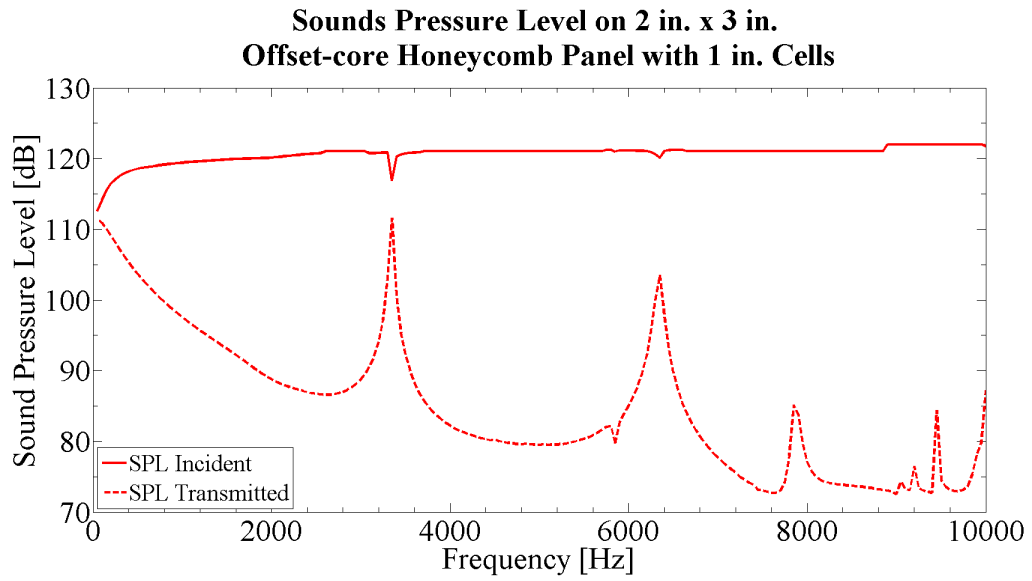


Figure 4.18: Sound pressure level on a 2in. x 3in. offset-core panel with 1in. cell size)

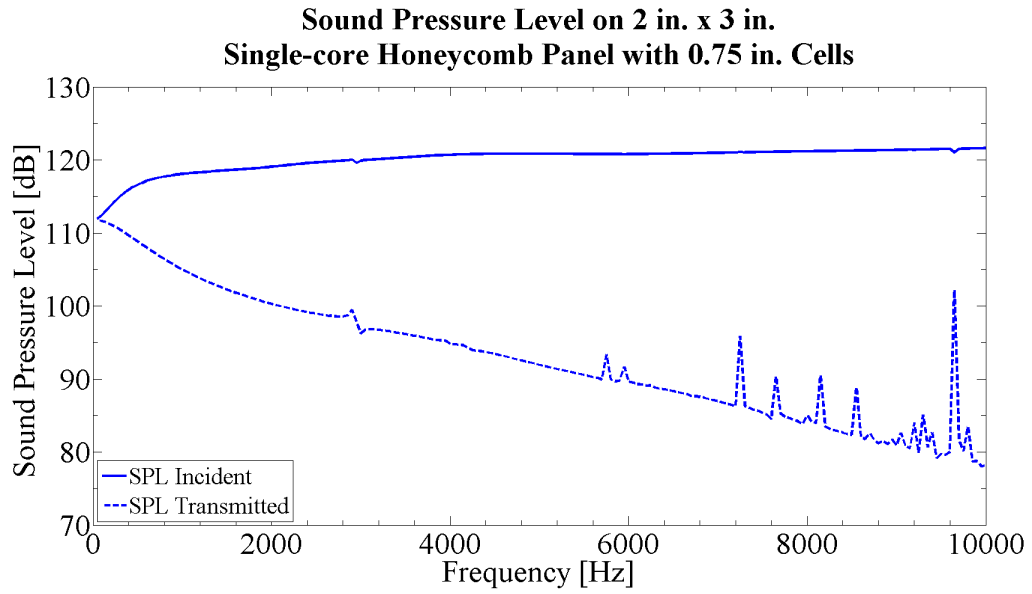


Figure 4.19: Sound pressure level on a 2in. x 3in. single-core panel with 0.75in. cell size)

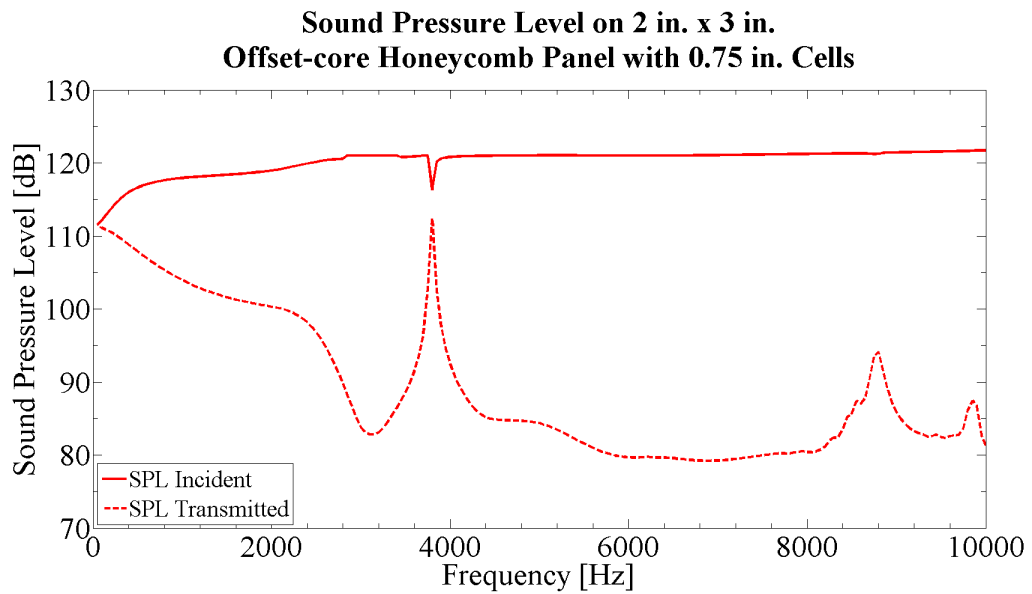


Figure 4.20: Sound pressure level on a 2in. x 3in. offset-core panel with 0.75in. cell size)

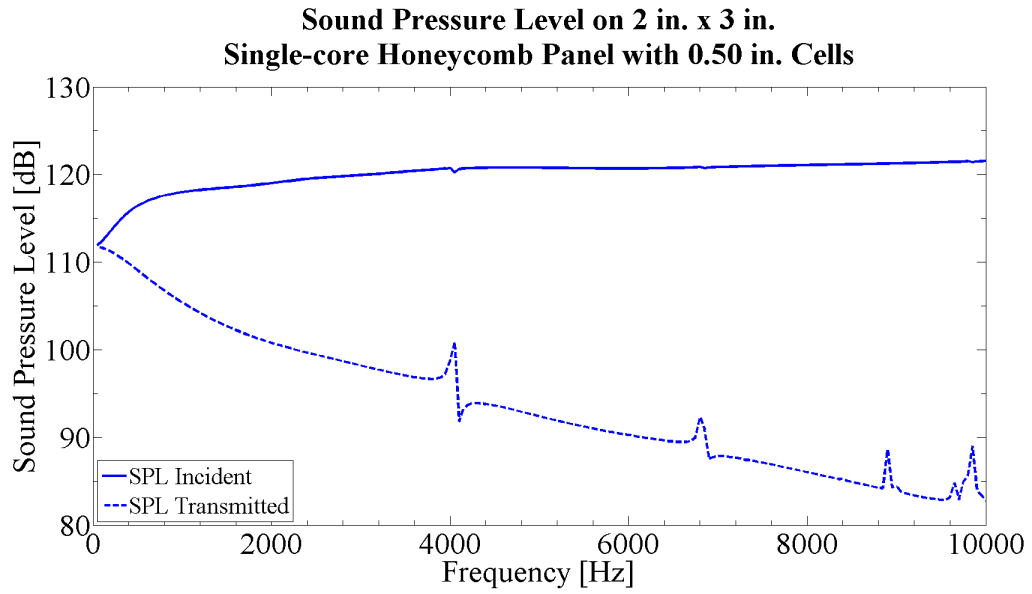


Figure 4.21: Sound pressure level on a 2in. x 3in. single-core panel with 0.50in. cell size)

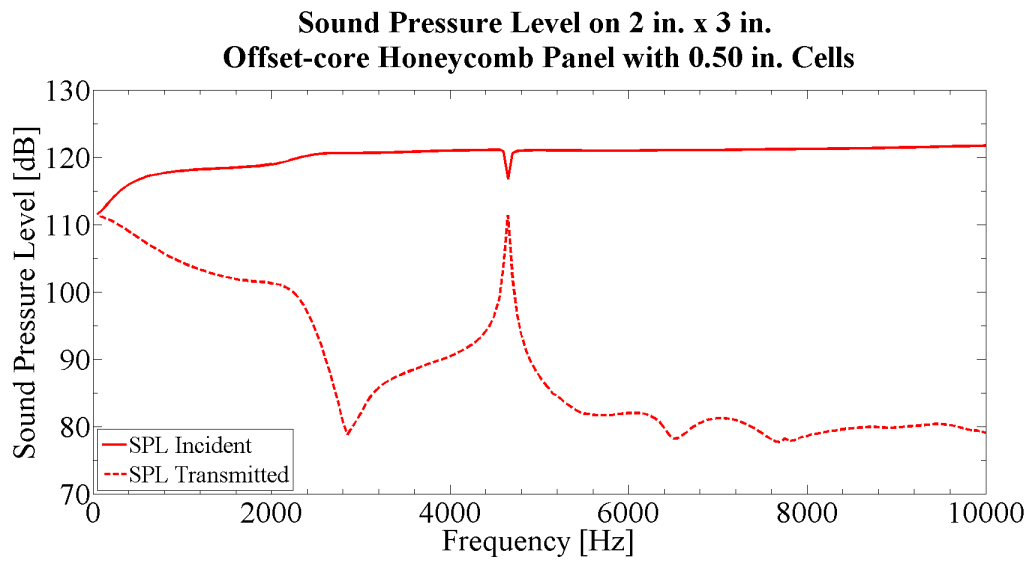


Figure 4.22: Sound pressure level on a 2in. x 3in. offset-core panel with 0.50in. cell size)

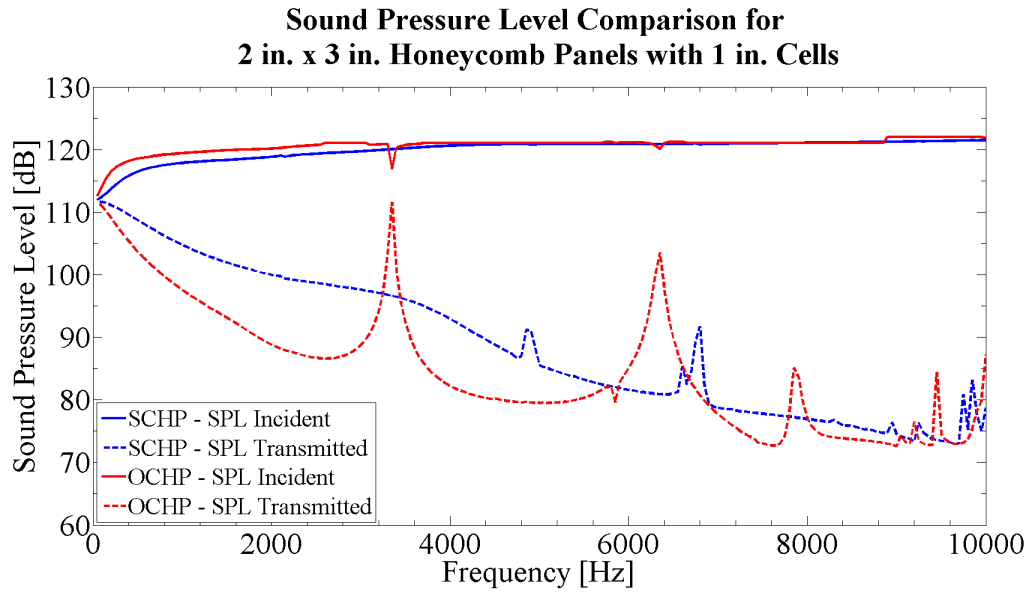


Figure 4.23: Sound pressure level comparison for 2in. x 3in. panels with 1in. cell sizes)

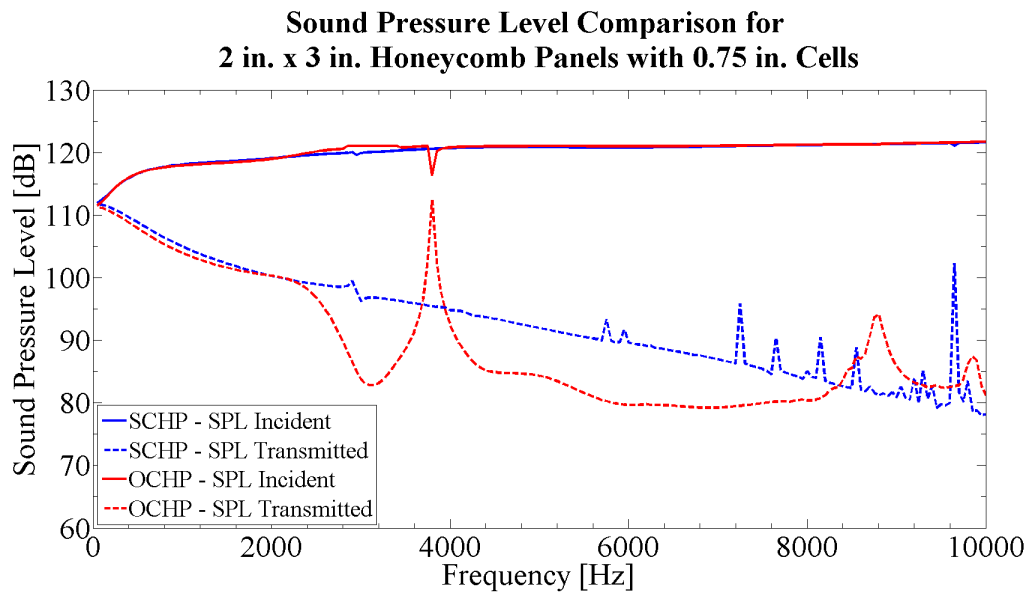


Figure 4.24: Sound pressure level comparison for 2in. x 3in. panels with 0.75in. cell sizes)

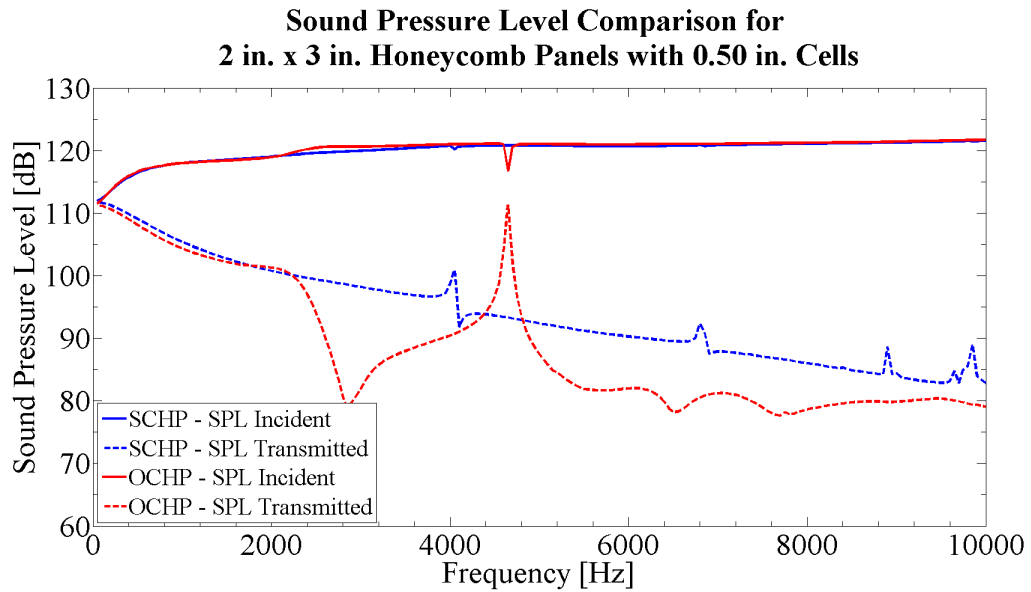


Figure 4.25: Sound pressure level comparison for 2in. x 3in. panels with 0.50in. cell sizes)

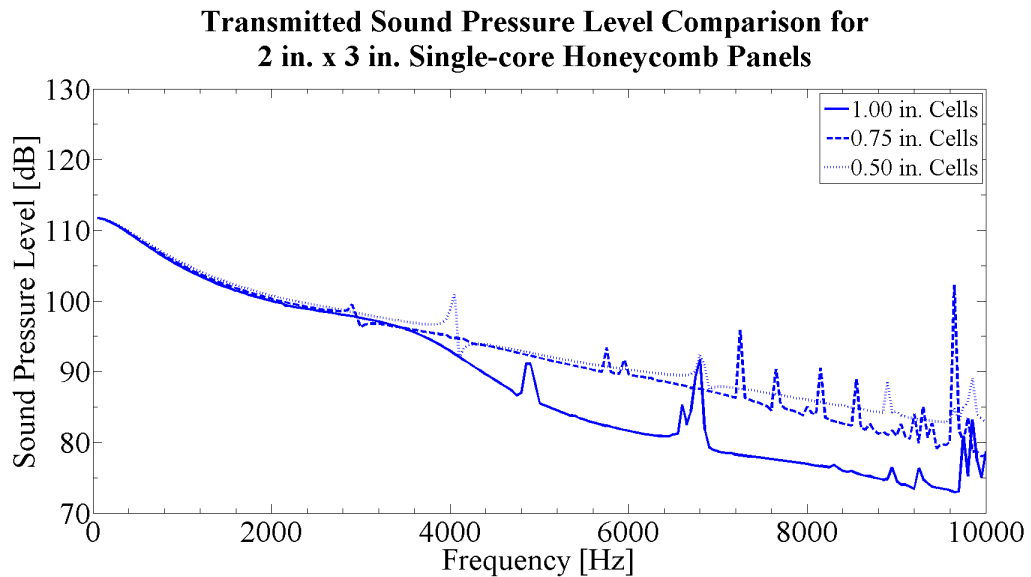


Figure 4.26: Sound pressure level comparison for single-core panels

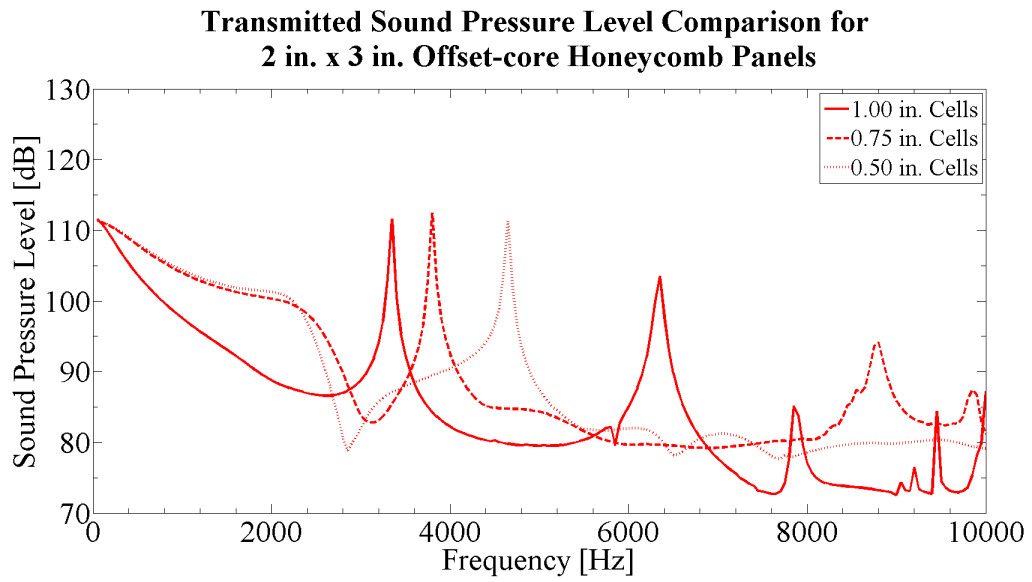


Figure 4.27: Sound pressure level comparison for offset-core panels

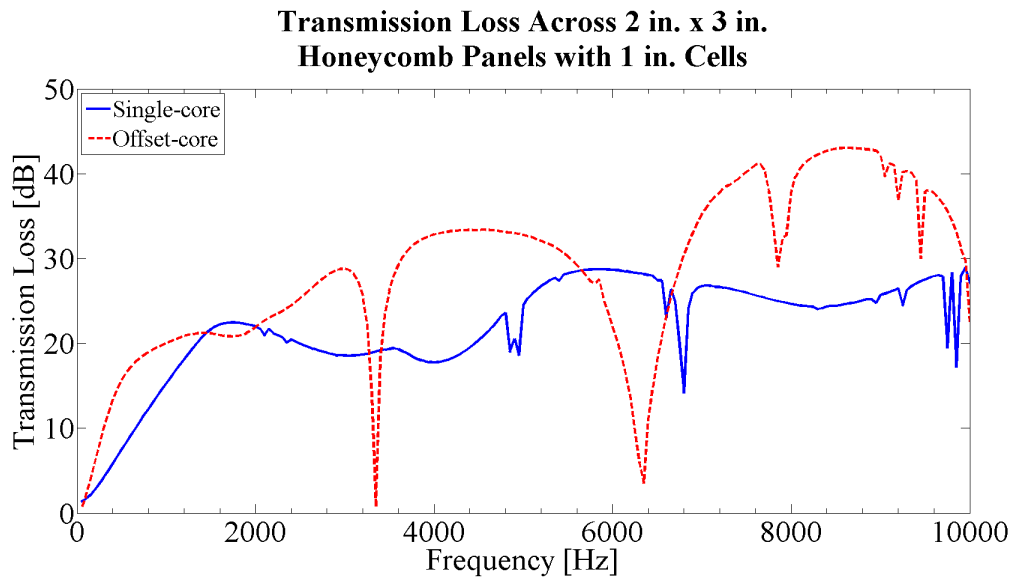


Figure 4.28: Comparison of transmission loss for 2in. x 3in. single-core and offset-core panels with 1in. cell size

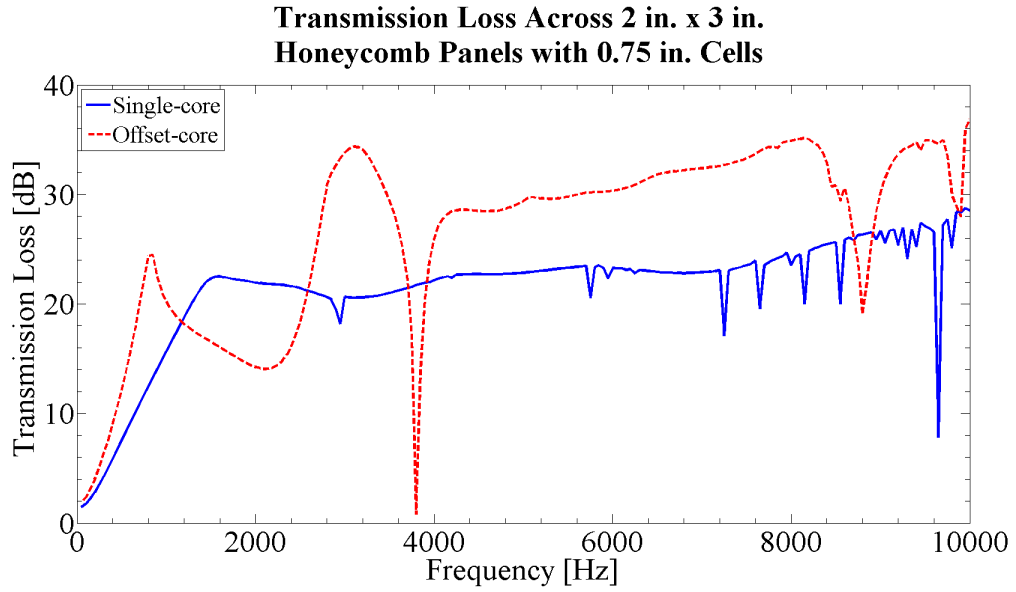


Figure 4.29: Comparison of transmission loss for 2in. x 3in. single-core and offset-core panels with 0.75in. cell size

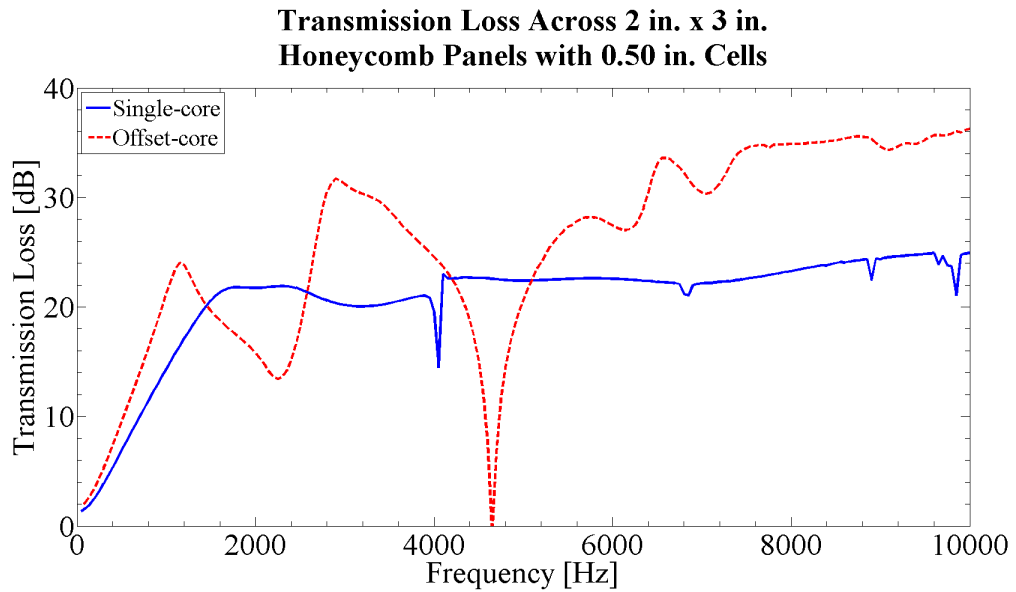


Figure 4.30: Comparison of transmission loss for 2in. x 3in. single-core and offset-core panels with 0.50in. cell size

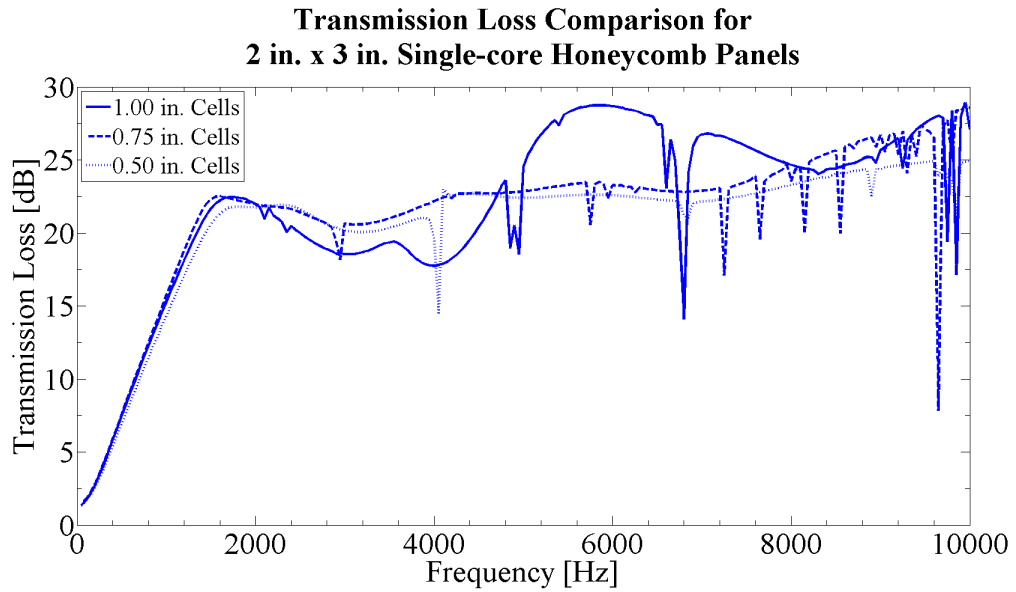


Figure 4.31: Comparison of transmission loss for single-core panels

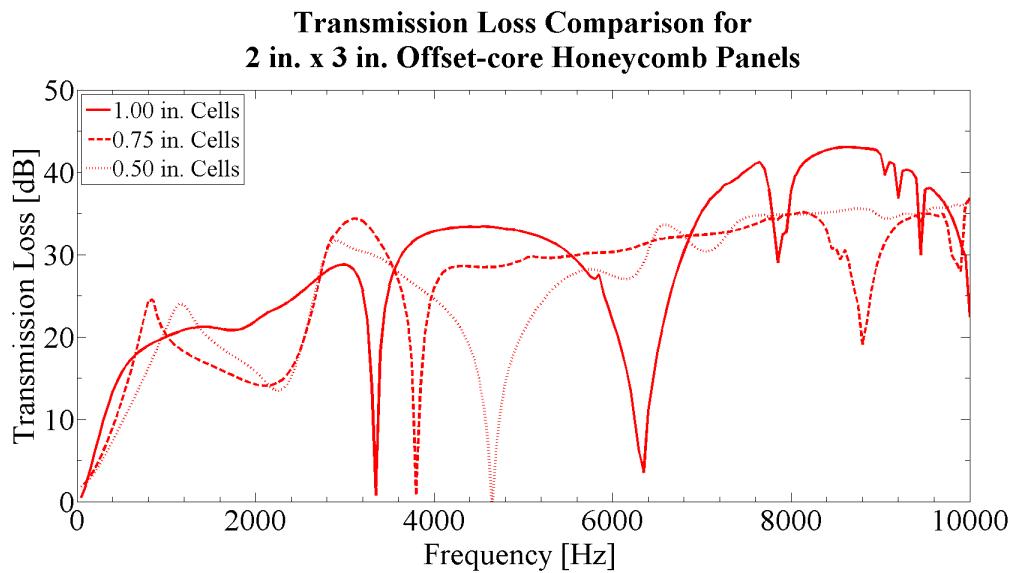


Figure 4.32: Comparison of transmission loss for offset-core panels

Table 4.3: Transmitted Overall Sound Pressure Level

a [in]	b [in]	S_T [in]	Type Core	Transmitted OASPL [dB]
2	3	0.50	SCHP	123.943
2	3	0.50	OCHP	123.182
2	3	0.75	SCHP	123.684
2	3	0.75	OCHP	122.856
2	2	1.00	SCHP	123.378
2	2	1.00	OCHP	120.469

CHAPTER 5

CONCLUSION

A discussion of acoustic-structure interaction, specifically in the case of honeycomb sandwich panels for impeding unwanted sound frequencies from propagating into an aircraft cabin, was provided. The FEA package, COMSOL Multiphysics, was benchmarked by comparing its solutions to those of theory for two relevant cases. Vibrational and acoustic-transmission models of single-core honeycomb sandwich panels and offset-core honeycomb sandwich panels were then developed with Solid Works. The models were analyzed with FEA in COMSOL Multiphysics, and several results were yielded:

- The first 24 natural frequencies of the SCHPs and OCHPs were found.
- The fundamental frequencies of each panel were found.
- The incident and transmitted sound pressure levels for each SCHP and OCHP were plotted and then compared.
- The transmitted OASPL for each SCHP and OCHP was calculated and tabulated.
- The TL across each SCHP and OCHP was plotted and then compared.

Transmission loss across the panels indicates that the offset-core honeycomb panels perform better than single-core honeycomb panels at noise reduction for a wide range of frequencies when the panel is impacted by a periodic wave at normal incidence. The results reported are an initial investigation of a relatively new instantiation of widely used technology, and they could be useful to any design engineers considering offset-core honeycomb panels.

CHAPTER 6

RECOMMENDATIONS

The work performed, thus far, focuses on the development and analysis of finite element models in an attempt to verify that an offset-core honeycomb sandwich panel can impede the propagation of sound, at various frequencies, more efficiently than a single-core honeycomb sandwich panel. The FEA models that were created, however, were rigid in their design. Future models could include parameterization so that cell length, cell width, cell depth, cell wall thickness, and face plate thickness could be quickly altered, and the model could be remeshed and resolved, with ease. Materials that are used for the honeycomb core and face plates could also be varied. Other core cell shapes, such as the columnar cells or compressed honeycomb cells, could also be explored. Boundary conditions, other than fixed face plate edges, could also be implemented.

In the case of TL, this thesis primarily focused on studies of acoustic waves impacting a panel at normal incidence. A study of acoustic waves impacting offset-core honeycomb panels at oblique incidence could produce useful results. It also has been shown that gas layers on the exterior of a sandwich panel can increase frequency-dependent TL through the panel due to impedance mismatch between gas layers and

the resulting inefficient energy transfer [54]. The inclusion of other gases within the cells of a honeycomb core may prove to affect TL at some frequencies. Higher frequencies could be explored with other numerical methods such as the energy finite element method [55] or statistical energy analysis.

Some offset-core panels have already been fabricated and studied, as discussed previously, but they have yet to be tested experimentally in an acoustic laboratory. Vibration studies could be performed with an electrodynamic shaker, and transmission loss studies could be performed by placing the offset-core panels in a frame between a reverberation room and an anechoic chamber. An experimental setup of this nature would allow one to study the panel's response to varying acoustic fields, i.e., plane waves, pseudorandom acoustic signals, swept sine waves, and mixed-mode signals. This experiment could also be conducted with the four microphone method by placing a portion of a test panel in the center of an impedance tube [56].

APPENDICES

APPENDIX A

MODAL ANALYSIS OF A RECTANGULAR PLATE

Rectangular Plate Natural Frequency Computation using Matlab

```
%% Material Properties
E = 70e9; % Young's Modulus [Pa]
nu = 0.33; % Poisson's Ratio
rho = 2700000; % Density [g/m^3]
a = 0.4064; % Length [m] = 16 [in]
b = 0.3048; % Width [m] = 12 [in]
h = 0.001016; % Height [m] = 0.04 [in]

%% Calculation
i = [1:1:6]; % Modes
j = [1]; % Modes

gam = rho*h % Mass per Unit Area [g/m^2]
D = ((E*h^3)./(12*(1-nu^2)))*1000 % Flexural Rigidity [Pa*m^3]
omega = pi^2*((i/a).^2+(j/b).^2).*sqrt(D/gam) % Angular Frequency [rad/s]
f(i,1) = omega./(2*pi) % Resonant Frequency [Hz]
```

Table A.1: Matlab Output for $f(i,j)$

$f(i,1)$	$f(i,2)$	$f(i,3)$	$f(i,4)$	$f(i,5)$	$f(i,6)$
41.7943	122.0393	255.7811	443.0195	683.7562	977.9864
86.9321	167.1772	300.9189	488.1573	728.8924	1023.1243
162.1619	242.4069	376.1486	563.3871	804.1222	1098.3540
267.4835	347.7285	481.4703	668.7087	909.4438	1203.6756
402.8970	483.1420	616.8838	804.1222	1044.8573	1339.0891
568.4024	648.6474	782.3892	969.6276	1210.3627	1504.5945

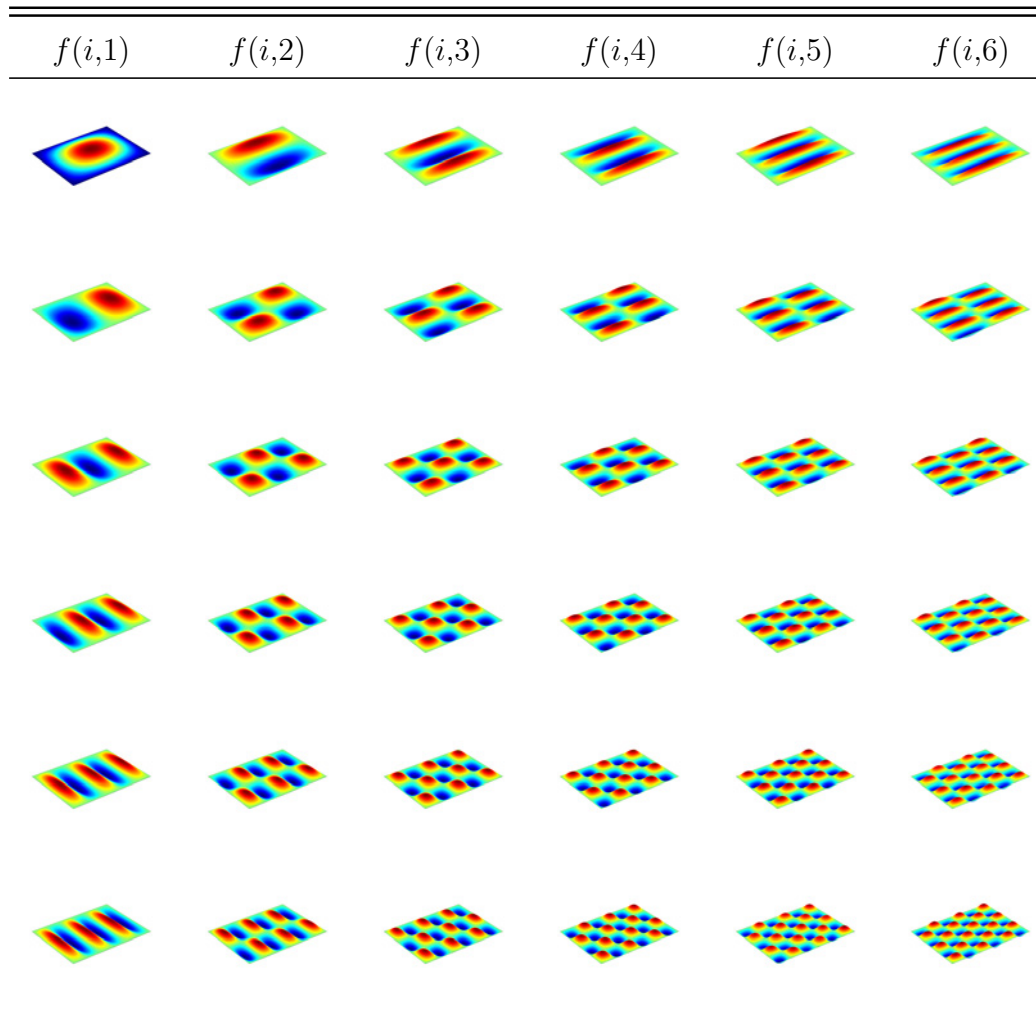
Table A.2: COMSOL Output for $f(i,j)$

$f(i,1)$	$f(i,2)$	$f(i,3)$	$f(i,4)$	$f(i,5)$	$f(i,6)$
41.7844	122.1103	256.2283	444.5072	687.4077	985.7573
86.9308	167.1920	301.2546	489.4852	732.2557	1030.5406
162.2652	242.4573	376.3868	564.4991	807.2041	1105.3122
267.9065	348.0159	481.7997	669.6735	912.2186	1210.2143
404.0495	484.0487	617.6480	805.2574	1047.3581	1344.9900
564.4991	650.7597	784.1423	971.4621	1213.2100	1510.1419

Table A.3: Percent Error Between Theory and COMSOL Results for $f(i,j)$

$f(i,1)$	$f(i,2)$	$f(i,3)$	$f(i,4)$	$f(i,5)$	$f(i,6)$
0.0237	0.0582	0.1748	0.3358	0.5340	0.7946
0.0015	0.0089	0.1116	0.2720	0.4614	0.7249
0.0637	0.0208	0.0633	0.1974	0.3833	0.6335
0.1581	0.0827	0.0684	0.1443	0.3051	0.5432
0.2861	0.1877	0.1239	0.1412	0.2393	0.4407
0.6867	0.3256	0.2241	0.1892	0.2352	0.3687

Table A.4: Displacement Plots for COMSOL Output of Natural Frequencies $f(i,j)$



APPENDIX B

MODAL ANALYSIS FOR HONEYCOMB SANDWICH PANELS

Table B.1: Displacement Field Plots for COMSOL Output of Eigenmodes for Offset Honeycomb $f(i,j)$

4 in. x 6 in.

Offset-core

$f(i,1)$

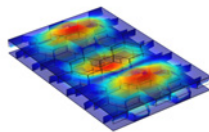
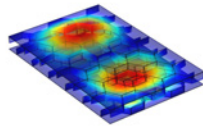
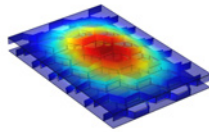


Table B.2: Natural Frequencies for Single-core Honeycomb Sandwich Panels - 2in. x 3in.

2in. x 3in. 0.5in. Cell	2in. x 3in. 0.75in. Cell	2in. x 3in. 1.0in. Cell
9629.91	7367.01	5399.92
12381.95	8832.65	5932.18
15752.63	9663.71	5970.21
16477.04	9705.09	6000.97
17833.06	0761.17	6384.87
18717.55	10207.99	6540.43
19359.87	10215.40	9247.06
20009.01	10383.90	9845.09
20026.00	10389.00	10677.21
20537.26	10581.89	10912.87
20539.59	10628.37	10936.00
20762.49	11118.99	11266.57
20927.48	11698.87	11399.01
21085.36	12142.74	11520.96
21085.53	16171.71	11627.36
21125.43	16210.03	11793.78
21173.35	16962.22	12136.41
21188.88	17595.74	12233.49
21828.62	17890.41	12569.74
21854.17	18557.22	12591.94
22143.89	18581.05	12885.99
22183.48	19210.56	12935.30
22186.10	19375.25	13491.58
22248.36	19630.83	14009.46

Table B.3: Natural Frequencies for Offset-core Honeycomb Sandwich Panels - 2in. x 3in.

2in. x 3in. 0.5in. Cell	2in. x 3in. 0.75in. Cell	2in. x 3in. 1.0in. Cell
4481.53	3785.81	3363.38
5050.11	4793.86	3843.88
5208.93	4799.36	3962.79
5259.23	3864.87	4027.60
5383.49	4873.54	4382.55
5395.06	6107.38	5050.85
6707.44	6192.61	5789.25
7532.90	6214.61	5833.42
8472.60	6215.49	5990.72
8483.66	6267.07	6131.58
8486.03	8323.20	6290.97
8493.05	8500.96	6942.08
8501.93	8508.48	7081.19
8507.74	8513.40	7137.78
8511.03	8522.18	7216.34
8515.52	8540.97	7237.29
8518.52	8548.75	7257.09
8532.63	8554.02	7271.22
8779.45	8594.89	7317.70
8789.48	8600.50	7391.79
8788.86	8610.79	7477.11
8790.42	8616.77	7838.86
8822.22	8633.31	7924.18
8830.76	8643.70	8267.30

Table B.4: Natural Frequencies for Single-core Honeycomb Sandwich Panels - 1in. Cell Size

2in. x 3in.	4in. x 6in.	8in. x 12in.
5399.92	3356.22	962.40
5932.18	4415.81	1318.92
5970.21	5802.35	1430.79
6000.97	6046.44	1476.02
6384.87	6704.68	1622.86
6540.43	7181.18	1691.59
9247.06	7567.56	1725.66
9845.09	8331.66	1841.59
10677.21	8350.65	1867.26
10912.87	8514.08	2328.51
10936.00	8775.51	2619.91
11266.57	8928.60	2685.92
11399.01	9070.06	2848.14
11520.96	9366.95	2982.52
11627.36	9472.58	2995.92
11793.78	9609.71	3185.09
12136.41	9825.62	3249.58
12233.49	10247.54	3260.55
12569.74	10309.27	3264.68
12591.94	10467.98	3291.25
12885.99	10687.29	3589.50
12935.30	10728.89	3602.98
13491.58	10990.59	3775.36
14009.46	11210.90	3813.90

Table B.5: Natural Frequencies for Offset-core Honeycomb Sandwich Panels - 1in. Cell Size

2in. x 3in.	4in. x 6in.	8in. x 12in.
3363.38	1153.59	824.33
3843.88	1883.82	1208.43
3962.79	2817.97	1673.15
4027.60	3006.53	1985.46
4382.55	3492.22	2377.44
5050.85	4115.55	2427.01
5789.25	4129.63	2470.01
5833.42	4130.21	2601.88
5990.72	4184.08	2669.12
6131.58	4400.35	2797.42
6290.97	4544.19	3180.25
6942.08	5189.07	3436.07
7081.19	5337.46	3593.72
7137.78	5757.08	4053.74
7216.34	5767.21	4318.08
7237.29	5821.51	4376.39
7257.09	5890.15	4405.74
7271.22	6590.33	4523.22
7317.70	6792.94	4626.07
7391.79	6813.47	4627.44
7477.11	6877.60	4676.86
7838.86	6908.65	4838.81
7924.18	6915.40	4848.66
8267.30	6928.89	4851.13

APPENDIX C

SOUND TRANSMISSION LOSS THROUGH A RECTANGULAR PLATE

Rectangular Plate Transmission Loss using Matlab

```
%% Material Properties

c_al = 6420; % Speed of sound in aluminum [m/s]
c_air = 343.2; % Speed of sound in air [m/s]
rho_al = 2700000; % Density of aluminum [g/m^3]
rho_air = 1275.4; % Density of air [g/m^3]
h_al = 0.001016; % Width of aluminum [m]

%% Acoustic Properties

r_al = rho_al*c_al; % Impedance of aluminum [(Pa*s)/m]
r_air = rho_air*c_air; % Impedance of air [(Pa*s)/m]
f = [50:50:5000]; % Frequency [Hz]
omega = 2*pi*f; % Angular frequency [rad/s]
k_al = omega/c_al; % Wave number of aluminum [(rad*m)/s^2]
```

```

%% Sound Intensity Transmission Coefficient

TIM = 4./(2+(r_air/r_al+...
    r_air/r_al)*(cos(k_al.*...
    h_al)).^2+(r_al^2/(r_air*z_air)...
    +(r_air*z_air)/r_al^2).*...
    (sin(k_al.*h_al).^2));           % Sound int. trans. coefficient

%% Plot

figure(1)

plot(f,TIM)

hold on

plot(f,TIC')

title('Transmission Through Aluminum'); % Plot title

xlabel('Frequency [Hz]');           % Label x-axis

ylabel('Transmission Coefficient'); % Label y-axis

```

REFERENCES

- [1] M. Pierucci. Effect of a transition layer on acoustic transmission from a fluid to an elastic layer. *Journal of the Acoustical Society of America*, 81(5):1630–1633, 1987.
- [2] J. Blackmon. Insulation system having vacuum encased honeycomb offset panels, 2005.
- [3] P.R. Cunningham and R.G. White. Dynamic response of doubly curved honeycomb sandwich panels to random acoustic excitation. *Journal of Sound and Vibration*, 264(3):579–603, 2003.
- [4] J.K. Paik, A.K. Thayamballi, and G.S. Kim. The strength characteristics of aluminum honeycomb sandwich panels. *Thin-walled Structures*, 35(3):205–231, 1999.
- [5] R. Zhou and M. Crocker. Sound transmission loss of foam-filled honeycomb sandwich panels using statistical energy analysis and theoretical and measured dynamic properties. *Journal of Sound and Vibration*, 329(6):673–686, 2010.
- [6] R. Zhou and M. Crocker. Boundary element analyses for sound transmission loss of panels. *Journal of the Acoustical Society of America*, 127(2):829–840, 2010.
- [7] R. Navaneethan. Study of noise reduction characteristics of multilayered panels and dual pane windows with helmholtz resonantors. Progress Report Contract KU-FRL-417-16, NASA, Marshall Space Flight Center, May 1981.
- [8] Stephen B. Horowitz. *Design and Characterization of Compliant Backplate Helmholtz Resonantors*. Master’s thesis, The University of Florida, 2001.
- [9] H. Denli and J.Q. Sun. Structural-acoustic optimization of sandwich cylindrical shells for minimum interior sound transmission. *Journal of Sound and Vibration*, 316(1-5):32–49, 2008.
- [10] W. Buhler and A. Frendi. Effect of fluid wall shear stress on nonlinear beam vibration. *Journal of Sound and Vibration*, 270(4-5):793–811, 2004.
- [11] A. Frendi. On the effects of wall shear stress on structural vibrations. *AIAA Journal*, 39(4):737–740, 2001.

- [12] A. Frendi. On flow unsteadiness induced by structural vibrations. *Journal of Sound and Vibration*, 269(1):327–343, 2004.
- [13] T. Abhijit and A. Frendi. Effect of decoupled fluid loading on nonlinear vibration of a flat plate. *Journal of Sound and Vibration*, 19:1117–1128, 2004.
- [14] A. Al Musleh and A. Frendi. On the effect of a flexible structure on boundary layer stability and transition. *Journal of Fluids Engineering*, 133(7):1–6, 2011.
- [15] A. Frendi. On the coupling between a supersonic turbulent boundary layer and a flexible structure. *AIAA Journal*, 35(1):58–66, 1997.
- [16] A. Frendi and L. Maestrello. On the combined effect of mean flow and acoustic excitation on structural response and radiation. *Journal of Vibration and Acoustics*, 119:448–456, 1997.
- [17] A. Frendi and L. Maestrello. Coupling between plate vibration and acoustic radiation. *Journal of Sound and Vibration*, 117(2):207–226, 1994.
- [18] A. Frendi and J. Robinson. On the effect of acoustic coupling on random and harmonic plate vibrations. *AIAA Journal*, 31(11):1992–1997, 1993.
- [19] L. Maestrello, A. Frendi, and D.E. Brown. Nonlinear vibration and radiation from a panel structure with transition to chaos induced by acoustic waves. *AIAA Journal*, 30(11):2632–2639, 1992.
- [20] A. Frendi and L. Maestrello. On the coupling between a supersonic boundary layer and a flexible structure. *AIAA Journal*, 31(4):708–713, 1993.
- [21] Rajesh Arjunan. *Vibroacoustic Parametric Analysis of Honeycomb Composite Fuselage for Improved Transmission Loss*. Master’s thesis, The University of Madras, 2002.
- [22] G. Kurtze and B.G. Watters. New wall design for high transmission loss or high damping. *Journal of the Acoustical Society of America*, 31(6):739–748, 1959.
- [23] C.F. Ng and C.K. Hui. Low frequency sound insulation using stiffness control with honeycomb panels. *Applied Acoustics*, 69(4):293–301, 2008.
- [24] S. Woody and S. Smith. Damping of a thin-walled honeycomb structure using energy absorbing foam. *Journal of Sound and Vibration*, 291(1-2):491–502, 2006.
- [25] E. Balmes and C. Florens. Validation of a vibration and electric model of honeycomb panels equipped with piezoelectric patch actuators. *Journal of Composites and Advanced Materials*, 19(3):319–338, 2009.
- [26] J. Kindinger. Lightweight structural cores. Technical report, Hexcel Composites, Connecticut, 2001.

- [27] Amit K. Jha. *Free Vibration Analysis of Sandwich Panel*. Master's thesis, National Institute of Technology Rourkela, 2007.
- [28] T.N. Bitzer. *Honeycomb Technology: Materials, Design, Manufacturing, Applications, and Testing*. Chapman and Hall, New York, 1st edition, 1997.
- [29] H. Wen-chao and N.. Chung-fai. Sound insulation improvement using honeycomb sandwich panels. *Applied Acoustics*, 53(1-3):163–177, 1998.
- [30] E. Ahmed and W.H. Wan Badaruzzaman. Evaluation of natural frequency and damping of profiled steel sheet dry board composite panel. *Journal of Engineering Science and Technology*, 6(6):695–708, 2011.
- [31] G. Kurtze and B.G. Watters. Panel and the like of high acoustic transmission loss, 1963.
- [32] E. Davis. Designing honeycomb panels for noise control. In *15th Aerodynamic Decelerator Systems Technology Conference*, number AIAA 99-1917, Toulouse, France, June 08-11 1999. American Institute of Aeronautics and Astronautics.
- [33] D. Palumbo and J. Klos. Development of quiet honeycomb panels. Technical Report NASA/TM-2009-215954, NASA, Langley Research Center, December 2009.
- [34] L. Barisciano. Broadband transmission loss due to reverberant excitation. Technical report, NASA, Langley Research Center, 1999.
- [35] M. Meo, A.J. Morris, R. Vignjevic, and G. Marengo. Numerical simulations of low-velocity impact on an aircraft sandwich panel. *Composite Structures*, 62(3-4):353–360, 2003.
- [36] R. Harish and R. Sharma. Vibration response analysis of honeycomb sandwich panel with varying core height. *International Journal of Emerging Technologies in Computational and Applied Sciences*, 6(1):582–586, 2012.
- [37] L. Jiang, K.M. Liew, M.K. Lim, and S.C. Low. Vibratory behaviour of delaminated honeycomb structures: A 3-d finite element modeling. *Computers and Structures*, 55(5):773–788, 1995.
- [38] C.C. Foo, G.B. Chai, and L.K. Seah. Mechanical properties of nomex material and nomex honeycomb structure. *Composite Structures*, 80(4):588–594, 2007.
- [39] S. Mohamady, R. Ahmad, A. Montazeri, R. Zahari, and Jalil N. Modeling and eigenfrequency analysis of sound-structure interaction in a rectangular enclosure with finite element method. *Advanced in Acoustics and Vibration*, pages 1–9, 2009.
- [40] M. Géradin and D. Rixen. *Mechanical Vibrations: Theory and Applications to Structural Dynamics*. Wiley, New Jersey, 2nd edition, 1997.

- [41] R.D. Blevins. *Formulas for Natural Frequency and Mode Shape*. Krieger Publishing Company, Florida, 1st edition, 2001.
- [42] B. Yang. *Stress, Strain, and Structural Dynamics: An Interactive Handbook of Formulas, Solutions, and MATLAB Toolboxes*. Elsevier Academic Press, London, 1st edition, 2005.
- [43] C.W. Silva. *Vibration: Fundamentals and Practice*. CRC Press, Florida, 2nd edition, 2006.
- [44] L.E. Kinsler, A.R. Frey, A.B. Coppens, and J.V. Sanders. *Fundamentals of Acoustics*. John Wiley and Sons, Inc., New York, 4th edition, 2000.
- [45] K. Tageman. *Modelling of Sounds Transmission Through Multilayered Elements Using the Transfer Matrix Method*. Master's thesis, Chalmers University of Technology, 2013.
- [46] W.S. Burton and A.K. Noor. Assessment of continuum models for sandwich panel honeycomb cores. *Computer Methods in Applied Mechanics and Engineering*, 145(3-4):341–360, 1997.
- [47] Andrew R. Staal. *Failure of Sandwich Honeycomb Panels in Bending*. Doctoral thesis, The University of Auckland, 2006.
- [48] A. Kayran and I. Aydincaak. Assessment of effective elastic properties of honeycomb cores by finite element analysis of sandwich panels. In *Proceedings of the 17th International Conference on Composite Materials*, Edinburgh, United Kingdom, 2009. International Conference on Composite Materials.
- [49] Z. Xue and J. Hutchinson. Crush dynamics of square honeycomb sandwich cores. *International Journal for Numerical Methods in Engineering*, 65(13):2221–2245, 2006.
- [50] Y. Tanimoto, T. Nishiwaki, T. Shiomi, and Z. Maekawa. A numerical modeling for eigenvibration analysis of honeycomb sandwich panels. *Composite Interfaces*, 8(6):393–402, 2001.
- [51] *COMSOL Multiphysics Reference Manual*, 2011.
- [52] S. Havaldar, R. Sharma, A. Antony, and M. Bangaru. Effect of cell size on the fundamental natural frequency of frp honeycomb sandwich panels. *Journal of Minerals and Materials Characterization and Engineering*, 11(7):653–660, 2012.
- [53] A. Boudjemai, M. Bouanane, Mankour, R. Amri, H. Salem, and B. Chouchaoui. Mda of hexagonal honeycomb plates used for space applications. *World Academy of Science, Engineering, and Technology*, 66:221–229, 2012.
- [54] C. Naify, C. Huang, M. Sneddon, and S. Nutt. Transmission loss of honeycomb sandwich structures with attached gas layers. *Applied Acoustics*, 72(2-3):71–77, 2011.

- [55] W. Zhang and S. Raveendra. High frequency vibro-acoustic analysis using energy finite element method. *SAE International Journal of Passenger Cars - Mechanical Systems*, 2(1):822–831, 2009.
- [56] S.S. Jung, Y.T Kim, and Y.B. Lee. Measurement of sound transmission loss by using impedance tubes. *Journal of the Korean Physical Society*, 53(2):596–600, 2008.